EIC Detector R&D Progress Report

The EIC Tracking and PID Consortium
(eRD6 Consortium)

December 29, 2018

The eRD6 Consortium

Project ID: eRD6

Project Name: Tracking & PID detector R&D towards an EIC detector

Period Reported: From July 2018 to December 2018

Project Leaders:

Brookhaven National Lab (BNL): Craig Woody
Florida Institute of Technology (FIT): Marcus Hohlmann
INFN Trieste: Silvia Dalla Torre
Stony Brook University (SBU): Klaus Dehmelt, Thomas Hemmick
Temple University (TU): Matt Posik, Bernd Surrow
University of Virginia (UVa): Kondo Gnanvo, Nilanga Liyanage
Yale University: Richard Majka, Nikolai Smirnov

Project Members:

BNL: B. Azmoun, A. Kiselev, J. Kuczewski, M. L. Purschke, C. Woody
BNL - Medium Energy Group: E. C. Aschenauer
FIT: M. Bomberger, M. Hohlmann
INFN Trieste: S. Dalla Torre, S. Levorato, F. Tessarotto
SBU: K. Dehmelt, A. Deshpande, P. Garg, T. K. Hemmick
TU: M. Posik, A. Quintero, B. Surrow
UVa: K. Gnanvo, N. Liyanage
Yale University: R. Majka, N. Smirnov

Contact Person: Kondo Gnanvo; kgnanvo@virginia.edu

Contents

1 Status of eRD6 Consortium and Future R&D Interests

The eRD6 and eRD3 were among the first original "consortia" funded for EIC Detector R&D for the development of EIC tracking and PID detectors beyond the present state-of-the-art technologies. After collaborating closely with eRD6, eRD3 recently merged fully into the eRD6 consortium. The consortium is leading the effort for the development of MPGD technologies for various Tracking and PID detector applications. The ongoing R&D efforts of the consortium focus on three core activities:

- *Development of large GEM detectors for EIC Forward Trackers:* This is a collaborative effort by Florida Tech, Univ. of Virginia and Temple Univ. to develop and test various readout foil designs (1D zigzag strips, 2D U-V strips, radial strips) with the goal to achieve excellent spatial resolution at low cost for large and low-mass GEM detectors. The groups have also developed different construction techniques for large-area GEM detectors that minimize the ratio of dead area to active area while also minimizing the material in the active area of these detectors.

- *Development of Fast TPC for the EIC Central Tracker:* This R&D is being conducted jointly by BNL, Stony Brook University and Yale University. It presently involves a broad effort that includes the development of new readout patterns (e.g., zigzag structures, 2D patterns, etc.), field cage design, ion backflow studies, prototype construction, readout electronics and calibration. It also brings in many aspects of R&D from other parts of our collaboration. In their last report, the Committee recommended that we put our TPC R&D plans more into focus. While we fully appreciate this recommendation and agree that eventually a more focused effort on a specific TPC design for EIC is required, we believe at this stage, it is still necessary to maintain a fairly broad investigation of the various technologies that will be needed in a final detector design. However, with the prospect of obtaining CD-0 approval for EIC in the not too distant future, we believe that it will soon be possible to concentrate on a more specific design in terms of detector size, magnetic field, resolution requirements and readout electronics which will allow us to better focus our efforts in this area.

- *Development of High Momentum RICH Detectors for EIC Hadron ID:* Several approaches are being investigated in this area. One such approach is being conducted by the SBU group with the development of a short length RICH with GEM-based photo detector. The group is also developing a process for the fabrication of large mirrors for RICH detectors. Another approach is the one pursued by INFN Trieste with the development of hybrid MPGD detectors combining THGEM photocathode and Micromegas amplification device with miniaturized pad readout for single photon detection applications.

The new R&D ideas that we plan to focus our future efforts on are:

- *R&D on μRWELL technology for tracking applications:* The interest in this novel technology within eRD6 spans across multiple institutions. Florida Tech, Temple U., and Univ. of Virginia plan to collaborate on the development of a cylindrical μRWELL detector that will provide fast hits to complement the slower TPC signals in the EIC central region, or that could be an alternative central tracker solution for a second EIC detector. The R&D challenge here is the implementation of both the cylindrical μRWELL amplification device and the readout structure on a foil instead of on a rigid PCB to develop a flexible detector that can be mounted on a low-mass cylindrical support structure. In a related effort, the BNL group plans to study the performance of a μRWELL structure combined with their zigzag readout development for the amplification and readout unit of the fast EIC TPC or other tracking detector applications.

- *Investigation of novel materials for RICH applications:* Another area of interest for the consortium is the study and development of new materials to enhance the performances of a high momentum RICH. SBU plans to investigate the speculative but highly promising transformation optical materials (TOMs) approach that could be tuned to match the Cerenkov effect in a way that would greatly help overcome the limitation of the current short length RICH. Meanwhile, INFN Trieste proposes to investigate the development of nano-diamond (ND) materials as an alternative to Cesium iodide (CsI) to improve the quantum efficiency of photocathodes of single photon detectors for high momentum RICH applications.

2 Past

2.1 Brief overview of project histories

2.1.1 Brookhaven National Lab

The group at BNL is mainly engaged in optimizing micro-pattern gaseous detectors (MPGD's) for reading out a time projection chamber (TPC) for use at the EIC.

Over the last few years we have built and tested numerous planar GEM detectors with long (˜16mm) and short (˜3mm) drift regions and have equipped them with both zigzag pad and straight strip readout geometries in an effort to study the spatial and angular resolution of a host of detector configurations. Following detailed studies of these detectors in the lab, beam tests were also carried out in 2012 and 2104 at Fermilab to fully characterize the performance of GEM detectors with extended drift gaps under beam conditions. The results of these efforts were published in a peer reviewed journal in 2014[1].

In addition, in collaboration with Stony Brook U. and Yale U., we have built a prototype combination TPC-Cherenkov (TPCC) detector to study the feasibility of performing tracking and pID measurements in a common detector volume. The detector was filled with a specially chosen gas to be used as both the Cherenkov radiator and the TPC working gas. After investigating important characteristics such as the drift velocity and the charge spread in various candidate gases, a beam test was conducted to demonstrate a proof of principle of the viability of this detector concept. The results from these tests were positive and are detailed in a manuscript recently submitted for publication in a peer reviewed journal (IEEE TNS). (Preliminary results from the TPCC have also already been presented at several conferences and have appeared in various conference proceedings[2].)

More recently we have focused on optimizing the design of the readout plane for a GEM detector made of zigzag shaped charge collecting anodes. We initially performed simulations to study the zigzag geometry, followed by a systematic set of measurements in the lab to reveal which geometrical parameters drive the performance of the readout. The results of these investigations were published in a peer review journal [3], with collaborators from Florida Tech and Stony Brook U.

The use of zigzag shaped anodes has been validated to a point that this R&D is considered complete for the eRD6 program. However, as part of a BNL funded LDRD, we continue to refine the design of the zigzag geometry by pushing the design parameters beyond what could be produced using standard chemical etching processes. A novel laser etching technique was used to generate PCB's with zigzag pad geometries with significantly finer features that more closely resemble idealized patterns determined by simulation. The first round of such laser etched PCB's were tested in the lab and very recently at a beam test at FNAL. A summary of these investigations was recently presented in a talk given at the 2018 IEEE NSS conference in Sydney, Australia.

Currently our focus is on investigating various avalanche technologies and anode geometries for a TPC readout, including the use of zigzag readouts with GEM's, Micromegas, μRWELL, and some combination of these. We have built a prototype TPC with zigzag readout and plan to employ our newly built cosmic ray telescope to study the reconstruction of particle tracks in the lab.

2.1.2 Florida Tech

The Florida Tech group has been focusing originally on the development of large low-mass GEM detectors with low channel count for the forward tracker (FT) of the EIC detector. In the current funding cycle the group has begun shifting focus towards R&D on cylindrical μRWELL detectors for a fast central tracker at an EIC detector.

We initially designed and implemented radial zigzag strips on large readout PCBs to achieve low-channel

count while maintaining good spatial resolution. We constructed a first one-meter-long prototype with such a readout at Florida Tech using a purely mechanical construction technique without any gluing and tested it in beams at Fermilab in 2013. This study showed a non-linearity in the position measurement of hits[4]. The reason was an over-etching of tips and under-etching of troughs in the zigzag strips, which caused insufficient interleaving of adjacent strips and consequently insufficient charge sharing among strips. We adjusted the zigzag strip design to improve the strip interleaving. Small PCBs and a flex-foil with the improved zigzag strip design were produced by industry and by CERN, respectively. We subsequently tested these with highly collimated X-rays at BNL. A substantial reduction in the non-linearity and an improvement in spatial resolution were observed[5].

Next, we designed a second large Triple-GEM detector that implements the drift electrode and a readout electrode with improved radial zigzag strips on polyimide foils rather than on PCBs to reduce the material in the active detector area[6]. These foils were then produced by CERN. To provide sufficient rigidity to this new detector while maintaining low mass, we produced the main support frames from carbon fiber material. We designed the GEM foils for this second detector in such a way that they can also be used for the second UVa FT prototype ("common GEM foil design"). A number of these GEM foil were produced for Florida Tech and UVa by the CERN workshop using the single-mask foil etching technique. Assembly of this second prototype showed that 3D-printed pull-out and frame components made from ABS did not have sufficient material strength to sustain the mechanical forces needed for stretching. They are now being replaced by stronger components made from PEEK.

A related effort on forward tracking detector simulations with EicRoot was begun in the previous funding cycle. We have also begun work with μRWELL detectors this funding cycle by assembling a planar $10\times10\,\mathrm{cm}^2$ μRWELL detector.

2.1.3 INFN Trieste

The task of the INFN participants to the eRD6 Consortium is "Further development of hybrid MPGDs for single photon detection synergistic to TPC read-out sensors".

Particle identification of electrons and hadrons over a wide momentum range is a key ingredient for the physics programme at EIC. One of the most challenging aspects is hadron identification at high momenta, namely above 6-8 GeV/c, where the only possibility is the use of Cherenkov imaging techniques with gaseous radiator. The overall constrains of the experimental set-ups at a collider impose a limited RICH detector length and to operate in magnetic fringing field. The use, for this RICH, of gaseous photon detectors is one of the most likely choice. The goal of our project is an R&D to further develop MPGD-based single photon detectors in order to establish one of the key components of the RICH for high momentum hadrons. This R&D has also some aspects synergistic to the development of TPC sensors: the miniaturization of the read-out elements and the reduction of the Ions Back-Flow (IBF).

The starting point are the hybrid MPGD detectors of single photons developed for the upgrade of the gaseous RICH counter [7, 8, 9, 10] of the COMPASS experiment [11, 12] at CERN SPS. These detectors are the result of several years of dedicated R&D [13, 14, 15, 16, 17, 18, 19, 20, 21, 22, 23, 24, 25, 26, 27, 28, 29, 30, 31]. They consists in three multiplication stages: two THick GEMs (THGEM) layers, the first one coated with a CsI film and acting as photocathode, followed by a resistive MicroMegas (MM) multiplication stage. The COMPASS photon detectors can operate at gains of at least 3×10^4 and exhibit an IBF rate lower than 5% [30, 32, 33, 34, 35]. An original element of the hybrid MPGD photon detector is the approach to a resistive MM by discrete elements: the anode pads facing the micromesh are individually equipped with large-value resistors and the HV is provided, via these resistors, to the anode electrodes, while the micromesh is grounded. A second set of electrodes (pads parallel to the first ones) are embedded in the anode PCB: the signal is transferred by capacitive coupling to these electrodes, which are connected to the front-end read-out electronics.

The whole R&D project develops over several years and it includes further improvements of the hybrid MPGD-based photon detectors in order to match the requirements of high momenta hadron identification at

EIC and initial tests relative to the application in gaseous detectors of a novel photocathode concept, based on NanoDiamond (ND) particles [36].

2.1.4 Stony Brook University

SBU is concentrating on the study of Ion Backflow (IBF) for a TPC, a possible candidate for the central tracker in at least one of the EIC detectors for an EIC. Furthermore, the TPC for sPHENIX has the same physical size when used in, e.g., the BeAST EIC detector.

It has been shown that IBF will pose a problem in an EIC detector and that the ultimate EIC TPC device must do more than sPHENIX to achieve the same level of position distortion. Our approach is to investigate new structures in and around the multiplication stage that promise significant better performance when considering IBF.

SBU proposed in the latest funding cycle the investigation of a new detector concept that might allow to significantly enhance particle identification via the Cherenkov effect with the help of meta-materials.

SBU also is working on the final installation of a unit that allows to produce high quality large size mirrors for RICH applications. The project is ongoing and expected to be finalized in about two months.

2.1.5 Temple University

Temple University (TU) has been focusing mainly on completing the the assembly and characterization of the commercial triple-GEM detectors. This R&D work was carried over from the eRD3 + eRD6 merger. These commercial triple-GEM detectors follow the STAR FGT triple-GEM design [37], but use commercial GEM, HV, and readout foils that were produced by Tech-Etch. Additionally these detectors are investigating the use of Kapton spacer rings in place of the more traditional G10 spacer grids. We were able to identify the cause of the electrical short that led to excessive sparking in the first two commercial triple-GEM detectors that were built last summer. Using the remaining materials, we are able to build two more commercial triple-GEM detectors prototypes 3 and 4. The third detector has now been completely assembled and is undergoing characterization, while all foils for the fourth commercial triple-GEM have been stretched and glued to their respective frames. During the third and fourth detector assemblies we implemented a fix to prevent the same shorting that occurred in the first two triple-GEM detectors. This fix was verified with the third chamber that we built.

The EIC is likely to contain two detector stacks, each at a different IR, and it would be beneficial to not have two identical detector stacks. In an effort to find an alternative technology to a TPC, which will most likely be contained in one of the detector stacks, we are beginning to focus on some simulation work within the EicRoot framework to quantify alternate technology choices. In particular the use of an MPGD in μTPC mode as a replacement or in addition to a TPC. This simulation work is being done to evaluate the performance of such a detector in a second EIC detector stack. We now have the basic machinery in place which enables us to easily adjust the dead material, gas, drift gap size, number of hit points, and specify the hit point, radial, and transverse resolutions of the detector. Work has now just started to modify these parameters to simulate a realistic detector digitization. To determine the proper resolution parameters test beam data taken by BNL with a MPGD operating in μTPC mode using a COMPASS styled readout will be used. Ultimately this simulation work of the μTPC will be integrated into the simulation work that is being done at FIT relating to the forward MPGD tracking. This integration will allow for a full tracking simulation which covers the mid-rapidity region consisting of a vertex detector and a MPGD μTPC barrel detector, as well as the forward/backward regions consisting of tracking MPGD detectors.

2.1.6 University of Virginia

The focus at UVa is the development of high performance, large and low mass GEM detector for the forward region of an EIC detector. Our R&D at UVa shares some similarities with the development by the Florida Tech and by Temple U. groups but we are specifically focused on the development of large area GEM with two dimensional U-V strips readout with fine pitch to provide excellent spatial resolution in both radial and azimuthal direction. A first prototype of such detector was built and successfully tested at the Fermilab Test Beam Facility (FTBF) in 2013. The analysis of the test beam data fully validated the expected performances of the U-V strip readout and the results were published in [38].

We recently completed the second phase of the R&D with a design improvement of the U-V strips readout that pushes even further the spatial resolution capabilities in both r and ϕ directions. The new prototype was conceived around the "Common EIC GEM foil design" jointly developed by UVa, Florida Tech (FIT) and Temple University (TU). The prototype was successfully built and tested in test beam at Fermilab in June 2018. The analysis of the test beam data is ongoing.

In addition, we have also been testing new ideas such as the ultra low mass Chromium GEM foil to reduce even further the material budget of EIC forward GEM trackers and the development of the double-sided zebra connection scheme to provide an elegant solution for the fine pitch U-V strips readout layer. We anticipate that several of these innovative ideas will ultimately be integrated in the final design of the forward GEM trackers of an EIC detector. Next, we plan to collaborate with TU and FIT, to conduct a joint R&D effort on a new MPGD technology, the μRWELL device, that we view as an alternative to GEM or Micromegas and an ideal candidate for cylindrical tracking device in the barrel region of an EIC detector.

2.2 What was planned for this period?

2.2.1 Brookhaven National Lab

1. ***Cosmic ray telescope***: After the assembly and preliminary testing of our GEM-based cosmic ray telescope, all four layers were dismounted and shipped out to Fermilab to be used by our colleagues at UVA for their beam test last summer. At Fermilab the 4 layers were used as a reference tracker for other particle trackers under test, which essentially served as a successful commissioning run for the telescope. (Details of the UVA beam test may be found in later sections of this report.) For this funding cycle, we planned to re-mount the 4-layers into the cosmic ray stand and measure cosmic rays in the lab in conjunction with the newly built prototype TPC, which will also be placed in the cosmic ray stand, as the detector under test. At this early stage we did not anticipate doing any detailed studies of the TPC other than verifying that the telescope and TPC prototype find matching tracks.

2. ***TPC prototype***: We planned to complete the assembly and commissioning of our new TPC prototype detector, which reuses the 10cm x 10cm x 10cm field cage from our older TPCC detector. This prototype will be used to study various readout plane geometries (including zigzag shaped charge collecting anodes) as well as different avalanche technologies (including GEM, Micromegas, and μRWELL) in a TPC application. In the long term, we also plan to investigate the optimum gas mixture to be used with a particular readout pad geometry and avalanche scheme. In addition, we eventually plan to optimize the operating parameters (like field and voltage configurations) of interesting avalanche options with regard to important detector characteristics such as charge spread due to diffusion, attachment, and ion back flow.

3. ***Electronics for TPC readout***: We planned to read out the prototype TPC with different electronics in order to compare the performance in each case. Initially we planned to use our work-horse electronics: the SRS/APV25 system, which is readily available, but not exactly ideal for a TPC application. Ultimately, we planned to read out the TPC with the SAMPA and DREAM electronics, primarily because we now have access to this hardware, but more importantly because both are directly suitable for reading out a TPC.

4. ***Zigzag readout***: As mentioned above, progress on this R&D topic is no longer funded under eRD6, however this work continues as part of a BNL funded LDRD program. We briefly report on some of this work since it has a direct impact on some important aspects of the TPC R&D done through eRD6. In short, we are continuing the development and optimization of zigzag pad geometries of readout planes for GEM, Micromegas, and μRWELL detectors. In particular, we are pursuing zigzag designs with unprecedented feature sizes, which are generated using a novel laser ablation technique. At this stage of the research, we are focused on examining the microscopic features of the fabricated zigzag structure, including the gap width between neighboring zigzag electrodes and the gap trench depth and the overall topology. Ultimately we hope to discover how such microscopic features influence charge sharing and the overall detector performance.

2.2.2 Florida Tech

1. **Forward Tracker Prototype:** One goal for this funding period was to extract the performance characteristics of the low-mass prototype from the data that we hoped to collect at the Fermilab beam test and to present the results at conferences and in a publication. In addition, we wanted to perform additional measurements on the detector with X-rays at Florida Tech, e.g. gain curves.

2. **EIC Simulations:** Undergraduate Matt Bomberger was to continue his EIC simulations to investigate the impact that material budgets in the forward and backward regions will have on the overall EIC detector performance. Our goal was to have results from a realistic simulation of the forward tracker region by May 2019.

3. **μRWELL detector:** We planned to work closely with UVa on the design of a first prototype for a small cylindrical μRWELL detector. Finally, we were to assemble and commission a 10×10 cm^2 μRWELL prototype with zigzag-strip readout and characterise its performance using X-rays.

2.2.3 INFN Trieste

Activity planned in period July 2018 - December 2018

Two R&D items were foreseen in this period:

1. Concerning the novel prototype of **single photon detector by MPGD technologies with miniaturized pad-size** the completion of a set-up adequate for test beam studies, the test-beam exercise and the initial analysis of the data collected at the test beam;

2. Concerning the **innovative photocathode based on NanoDiamond (ND) particles**, the continuation of the initial studies to understand the compatibility of this photocathode type with the operation in gaseous detectors and, in particular, in MPGD-based photon detectors.

2018 milestones:

- September 2018: The completion of the laboratory characterization of the photon detector with miniaturized pad-size.

- September 2018: The performance of the tests to establish the compatibility of the ND photocathodes with the operation of MPGD-based photon detectors.

2.2.4 Stony Brook University

It was planned to continue the installation of an electron-ion beam system into the evaporator at SBU.

We were also planning analyzing the data taken with a TPC prototype in a test-beam campaign in June/July 2018 at the Fermilab Test Beam Facility (FTBF) and starting up the IBF measurements.

Furthermore, we were planning to start investigating the properties of meta-materials that were obtained via optical transformation methods.

2.2.5 Temple University

For this funding cycle TU has planned to complete the eRD3 carry over work that is listed below.

1. Determine shorting issue that was seen in the first two commercial triple-GEM detectors last summer.
2. Build two more commercial triple-GEM detectors using remaining GEM, HV, and readout foils, and correct the electrical shorting problem.
3. Verify the electrical shorting issue has been resolved.
4. Characterize the two newly built triple-GEM detectors.

In parallel to the above hardware work, we are also working on simulating a MPGD detector used in μTPC mode as a possible detector replacement/addition to a TPC in an EIC detector stack located at a second IR. Below lists several simulation goals that TU had set.

1. Develop machinery to simulate a μTPC detector, where dead material, gas, drift gap size, hit points, and resolution parameters can be easily adjusted.
2. Use test beam data from μTPC with COMPASS readout (taken by BNL) to implement realistic resolution parameters.
3. Develop more realistic detector digitization where the hit point resolution varies as a function of barrel radius (*i.e.* first and last hit point before readout could have different resolutions).
4. Once detector is fully simulated this and the forward MPGD simulation work being done by FIT can be integrated into one cohesive tracking simulation.

2.2.6 University of Virginia

For the current cycle, we planned to:

1. **Large EIC-FT-GEM prototype:** Analyze Fermilab 2018 test beam data. Continue the characterization of the prototype with cosmic and x-ray at UVa and at the BNL x-ray scan setup if required. Start drafting the manuscript for publication of the results in peer-reviewed journal.
2. **R&D on μRWELL detector technology:** Work closely with FIT on the design of a small cylindrical μRWELL detector. Study and characterize the current small prototype. Conduct R&D with the focus on low mass and high resolution 2D readout strips patterns.
3. **VMM readout Electronics:** Acquire a small size VMM-based Scalable Readout System (SRS) and test the electronics with the large GEM and μRWELL prototypes. Perform a comparison study of the performances of VMM-SRS readout system with the APV25 electronics.
4. **Draft paper on Chromium GEM (Cr-GEM) studies:** Pursue the study of the performance of Cr-GEMs with our existing prototype and draft a paper on the results of these studies for publication in NIMA or TNS journal.

2.3 What was achieved?

2.3.1 Brookhaven National Lab

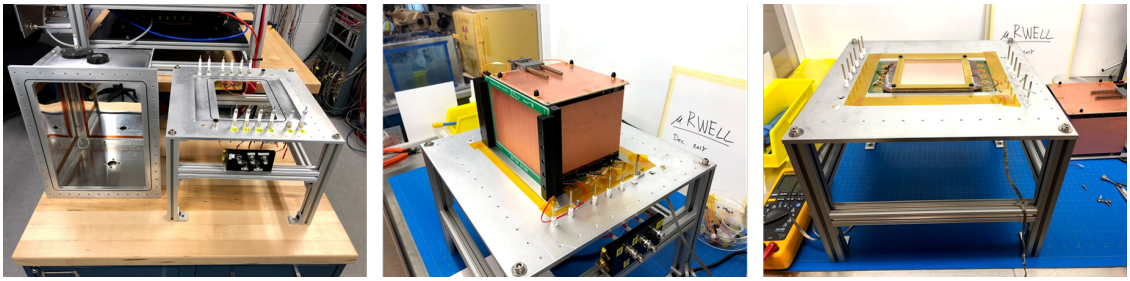

Figure 1: Photos of the TPC enclosure, base plate, field cage and GEM stack respectively.

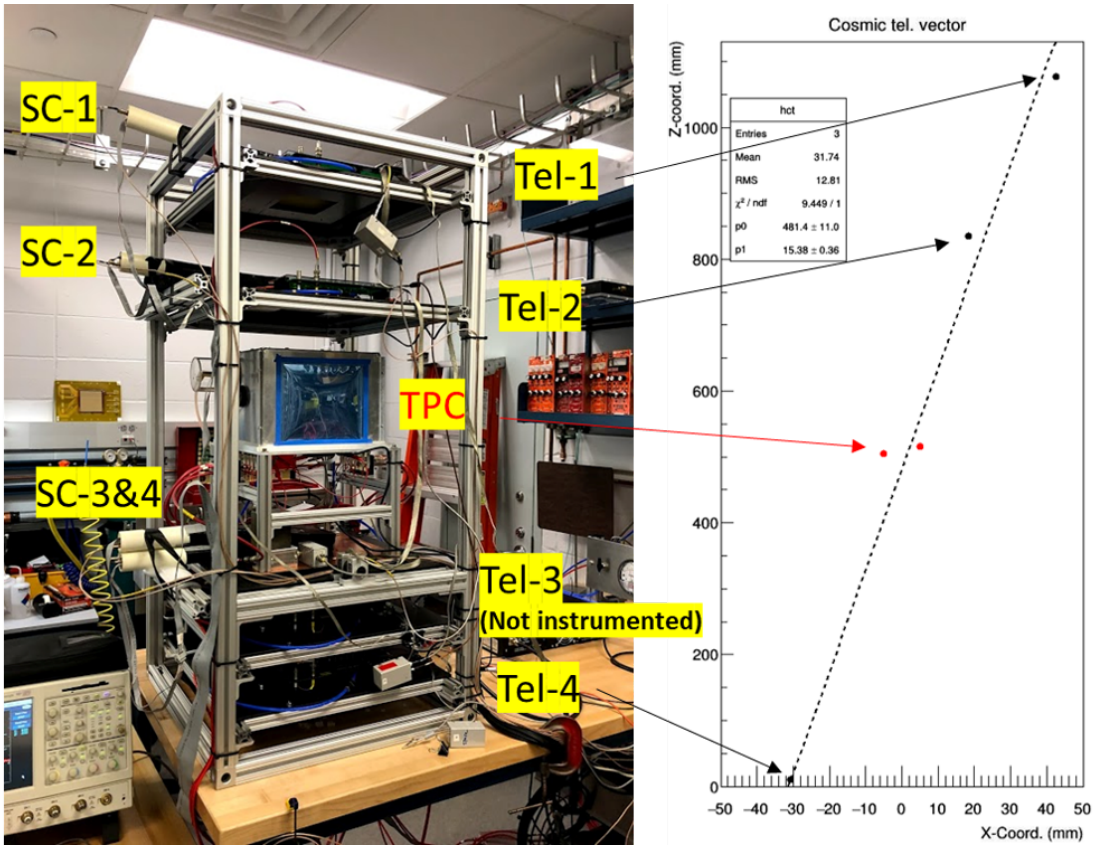

Figure 2: Photo of the cosmic ray stand holding 4 scintillation counters (SC 1-4), 4 GEM tracking layers (Tel 1-4), and the newly assembled TPC prototype. The plot on the right shows the reconstructed space points in each layer of the telescope (black) and the TPC (red). The particle vector in the X-Z plane is determined as a linear fit to these points.

1. ***Cosmic ray telescope***: After the four layers of the cosmic ray telescope were returned to BNL from the UVA group, they were remounted to the cosmic ray stand with HV, gas, and front end electronics all restored (see Fig. 2). Initially, the operation of each layer, consisting of a triple GEM coupled to a COMPASS style X-Y strip readout was verified by observing signals from an Fe55 source. Next, the telescope was tested by attempting to reconstruct cosmic ray tracks. The SRS/APV25 DAQ elecronics

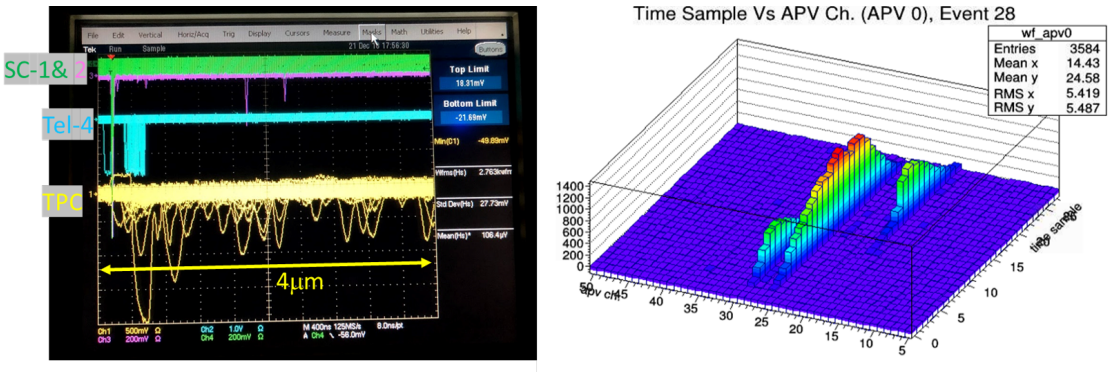

Figure 3: Left: scope traces from the scintillation trigger, a single telescope layer, and the TPC. Right: waveforms from fired pads of a single TPC event.

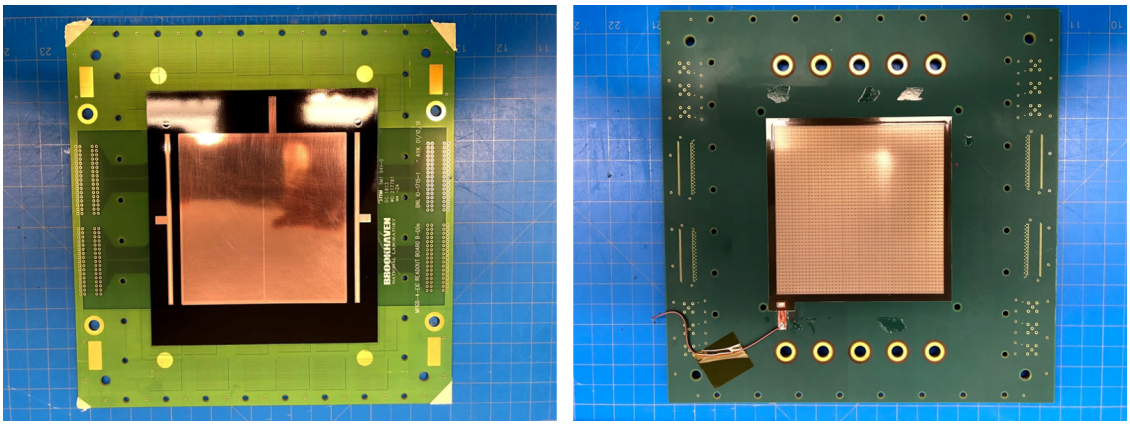

Figure 4: PCB with zigzag shaped anodes with a μRWELL coupled to it (left) and a similar PCB with a Micromegas coupled to it (right).

were used to read out the charge collected by the X-Y strips of each layer and a charge weighted mean (or centroid) was calculated along each coordinate. (In this case, only 3 of 4 layers were instrumented since the electronics for the fourth layer was needed for the TPC prototype.) As shown in Fig. 2, the three space points were then fit to a straight line to reconstruct the particle track. However, for the preliminary analysis only the raw data is plotted, with no lateral offsets applied to account for any misalignment of the different layers with respect to one another. Nonetheless, the single point resolution of each layer is typically known to be about 50-60μm for these kinds of planar trackers. Once all aspects of the system are calibrated, we expect the position resolution for fully reconstructed tracks to be between 50-60μm/sqrt(4 points) = 25-30μm, which should provide a suitable reference track for studying the TPC prototype.

2. ***TPC prototype***: The assembly and preliminary testing of the TPC prototype has been completed. The new gas enclosure was checked for leak tightness and the 20kV feed-through used to energize the top plate of the field cage, as well as the field cage itself passed stringent HV tests. Next, the field cage, GEM foils and readout PCB were all mounted to the aluminum base plate of the TPC (see Fig. 1) and the apparatus as a whole was found to be fully operational. To test the prototype, the detector was placed in the cosmic ray stand, as shown in Fig. 2 and a cosmic trigger was established using the coincident signal from four scintillation counters. As mentioned, the TPC was read out using SRS/APV25 DAQ electronics to measure particle tracks at slight inclinations to the readout plane. For the purpose of commissioning the setup, the TPC chamber was purged with ArCO2 (70/30), and the field cage was operated at 0.75kV/cm, resulting in a drift velocity of about 25μm/ns. This corresponds

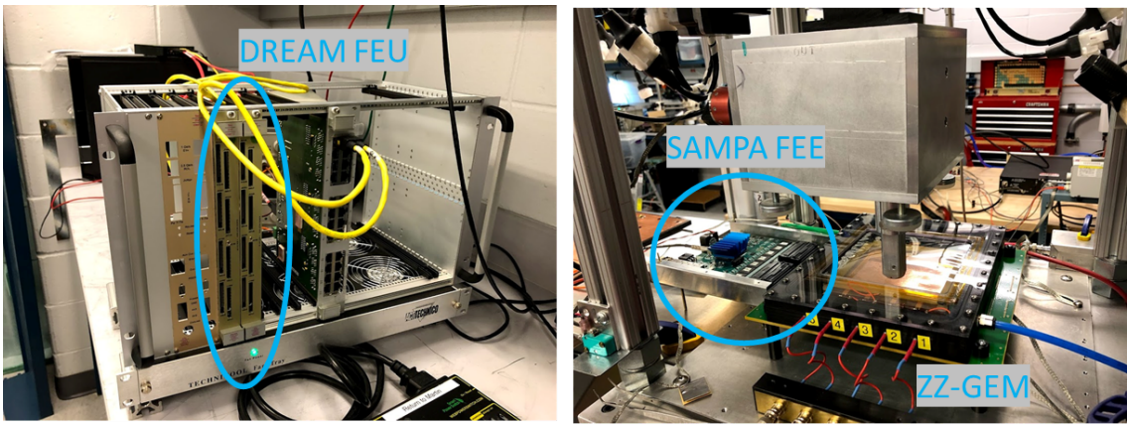

Figure 5: Photos of the DREAM electronics which require a 1-2m micro-coaxial cable to deliver the primary charge to the rack mounted front end FEU modules (left), and a SAMPA front end card connected directly to a planar GEM chamber with zigzag readout.

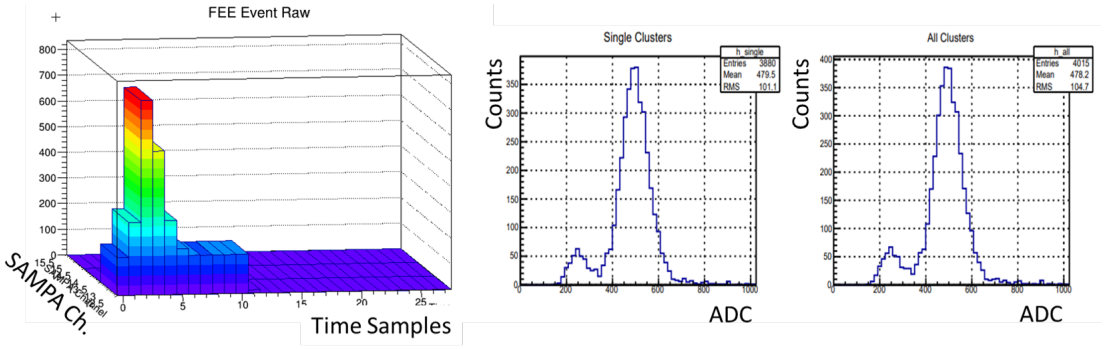

Figure 6: Waveforms recorded by the SAMPA front end card connected to a planar GEM detector (left) and the resulting pulse height spectrum from a Fe55 source (J. Kuczewski, BNL).

to a drift time of about 4μs over a 110mm drift distance. This can be seen in Fig. 3 which shows multiple scope traces from the output of a preamp-shaper AC-coupled to the bottom GEM foil of the TPC prototype, where the signals from primary clusters span a time frame of about 4μs. The other scope traces correspond to the prompt trigger from the scintillation counters and in-time signals from the bottom GEM foil of a single telescope layer. Since the DAQ electronics are only capable of collecting data for about 700ns per trigger, data for only a portion of the primary ionization in the drift volume is recorded. For this preliminary test, timing information from the waveforms of fired pads (see the right panel of Fig. 3) was used to determine the Z-coordinate, and the middle of the corresponding pad rows were taken to be the X-coordinate, again with no alignment corrections applied yet. While the electronics employed here are not ideal for studying the TPC, they allow us to demonstrate that the apparatus is operational. Ultimately, the raw reconstructed space points from the TPC were found to match the tracks reconstructed by the GEM telescope fairly well.

It should also be mentioned that we have received a zigzag readout PCB with a Micromegas coupled to it from CEA Saclay and a similar PCB with a μRWELL coupled to it from the gas detector shop at CERN (see Fig. 4). Though we will ultimately install these PCB's in the TPC prototype to evaluate their performance. we will initially study these avalanche schemes in a simple planar detector configuration, with a short drift gap.

3. ***Electronics for TPC readout***: Though we have not yet read out the TPC with the SAMPA or DREAM electronics, both are currently being tested in the lab with other setups and will soon be

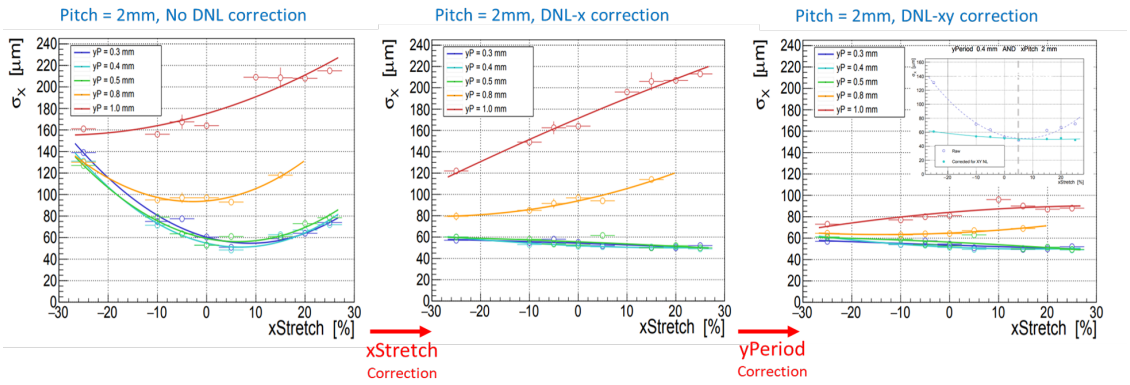

Figure 7: Beam test results of the position resolution of a 4-GEM coupled to a "multi-zigzag" patterned readout PCB (C. Perez, Stony Brook Univ.). The measured centroid suffers a deviation from linearity for large and small stretching parameters, and for large zigzag periods. The inset plot on the right compares the results for zigzag parameters where no correction for a differential non-linearity is required to a case where there is a large deviation from a linear response.

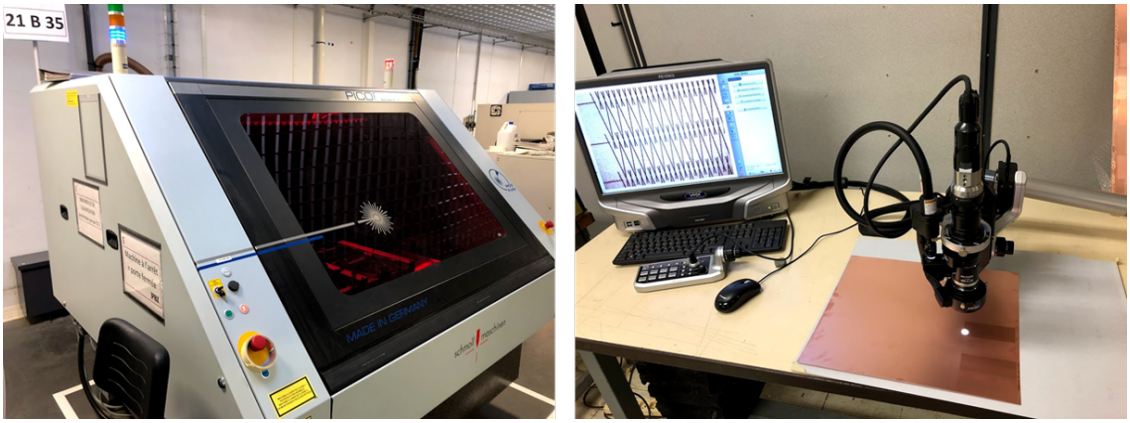

Figure 8: Photo of the laser ablation machine at Elvia in Coutances, France and the microscopic inspection of a laser etched PCB sample.

available for use by the TPC (see Fig. 5). In particular, we are working closely with a BNL electronics engineer (J. Kuczewski), who is developing the ASIC and firmware to read out the SAMPA chips. A SAMPA front end card (FEE) and data aggregation module (DAM) have already been developed to read out 8 SAMPA chips simultaneously (corresponding to 256 ch.). and were used successfully to read out a planar GEM with a zigzag readout, as shown by the preliminary results in Fig. 6. In addition, the DREAM electronics was successfully used at our last beam test (see below) to read out our GEM "multi-zigzag" patterned PCB's and will soon be available to read out the TPC. There is also ongoing work to integrate each set of electronics hardware into the RCDAQ DAQ framework used at BNL.

4. ***Zigzag readout***: As part of our ongoing work on zigzag readouts supported by LDRD funds, we have used laser ablation to produce a GEM readout PCB with zigzag shaped anodes with multiple patterns on a single board for the purpose of evaluating the performance of sensitive geometric parameters of the zigzag structure. The narrow beam diameter of the laser has allowed for the possibility to generate unprecedented feature sizes in the copper substrate, like space gaps between neighboring strips as narrow as 25μm or less, which has given us the ability to realize and test new and interesting zigzag patterns. As reported last time, several such PCB's were tested in a beam test at Fermilab last March. Now that the data analysis is complete, some compelling performance trends are beginning to emerge, as shown in Fig. 7. In this figure, the dependence of the position resolution on the zigzag period

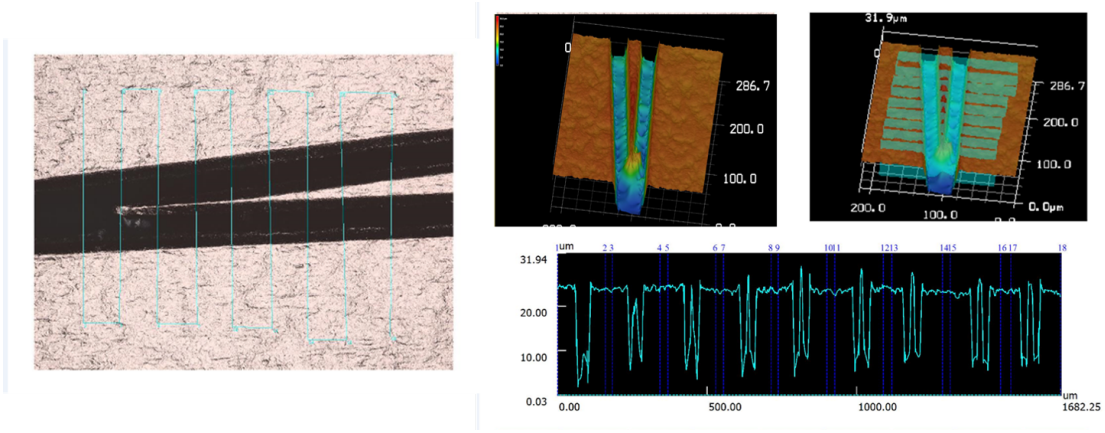

Figure 9: 3D analysis of the tip of a zigzag shaped anode of a readout PCB.

and the degree of zigzag interleaving (ie, the "x-stretch" parameter) is shown. For this particular application, the resolution appears to reach a minimum for a stretch parameter of around 5 percent and in general improves with smaller zigzag periods. In addition, the resolution appears to saturate at a period of around 0.5mm. Since the deviation from linearity (ie, the differential non-linearity (DNL)) is able to be measured as a function of the calculated centroid, the non-linearity may be corrected to recover the resolution found in the best performing patterns. Ultimately, a set of optimized zigzag parameters were identified where essentially no DNL correction is required, and where the resolution was found to be around 50μm for a 2mm pitch.

Since conducting the beam test, we have visited a PCB manufacturing facility in Coutances, France called Elvia that specializes in laser ablation. During the visit, we had the opportunity to work directly with a laser ablation machine (see Fig. 8) in an effort to optimize its working parameters, including the laser intensity and the number of laser passes over a given region of the design. By also carefully examining the micro-pattern structure of a laser etched PCB, we have revealed features like hair-thin copper traces (see Fig. 9) resulting from the incomplete trenching of the substrate by the laser, which is responsible for bridging neighboring pads and creating a short. Through such detailed inspection of the PCB's we can now take corrective steps in designing the zigzag pattern and can modify the instruction set for the machine to avoid such issues. More generally, with the ability to create micro-pattern structures on a readout plane with feedback from such microscopic inspection, we believe we can iterate on the fabrication procedure to provide a path to closely realizing the ideal zigzag designs originally suggested by simulation.

Publications:

1. A manuscript entitled, "Beam Test Results from a GEM-based Combination TPC-Cherenkov Detector" has been submitted to the peer reviewed journal, IEEE Transaction on Nuclear Science. Consortium members from Stony Brook University, Yale, and BNL are co-authors for this paper.

2. An oral presentation entitled, "Design Studies of High Resolution Readout Planes using Zigzags with GEM Detectors" discussing the results of the new zigzag PCB's produced using laser ablation was given at the 2018 IEEE NSS/MIC conference in Sydney, Australia last November.

2.3.2 Florida Tech

Refurbishment of low-mass EIC Forward Tracker GEM detector prototype: The 3D-printed ABS pieces used in the original construction of the prototype chamber tended to deform and crack under tension causing the foils separated by a 1 mm gap to short out due to a lack of overall tension in the GEM

stack. Consequently, we were not able to operate the prototype detector in the Fermilab beam test. We are replacing the ABS pieces with parts made from polyetheretherketone (PEEK), which is a polymer material with a tensile strength comparable to steel. Specifically, we are replacing the pull-outs that the GEM stack is tensioned against and two layers of inner frames. Fig.10 shows a test installation of the PEEK pull-outs in the detector.

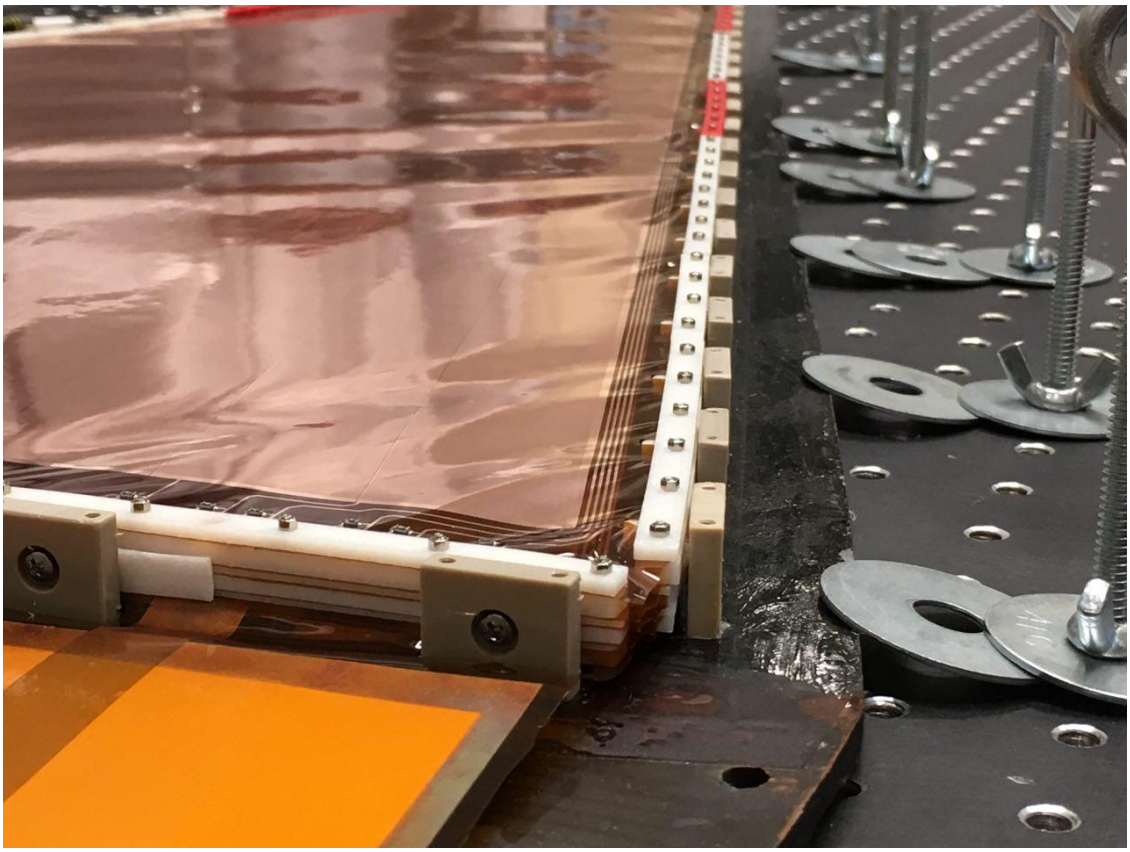

Figure 10: Installation of PEEK pull-outs (beige blocks) in the low-mass GEM prototype.

However, just as before we still observe shorts in the original GEM stack between those foils that are only 1 mm apart. To correct this, we increase the spacing between the closest foils in the GEM stack. Two new PEEK layers of inner frames with 2 mm thickness are now being implemented. This will result in a stack with 3-2-2-2 mm gaps (drift, transfer 1, transfer 2, induction) instead of the previous 3-1-2-1 mm spacing. The purely mechanical construction and stretching technique that we employ for this prototype allows this kind of retrofitting.

For producing the pull-out parts, a 12"×12" plate of 6 mm thick PEEK was machined on campus. In the original design of the inner frames, all pieces had the same short length of about 10 cm with 1 cm gaps between them. This resulted in warping of the GEM foils in the gaps. In the new design (Fig. 11), the side frames will be longer and fewer - more similar to the frame design of the CMS GE1/1 GEMs that this prototype is based on. The proper power setting of a laser cutter is currently being investigated for machining the inner frame pieces from a 12"×6" plate of 2 mm thick PEEK, which is too thin for cutting on an NC machine.

EIC Simulations: Undergraduate student Matt Bomberger continued his work on EIC simulations for investigating the impact that material budgets in the forward and backward regions will have on the overall EIC detector performance. He went to BNL in early August for a week to work directly with EicRoot expert

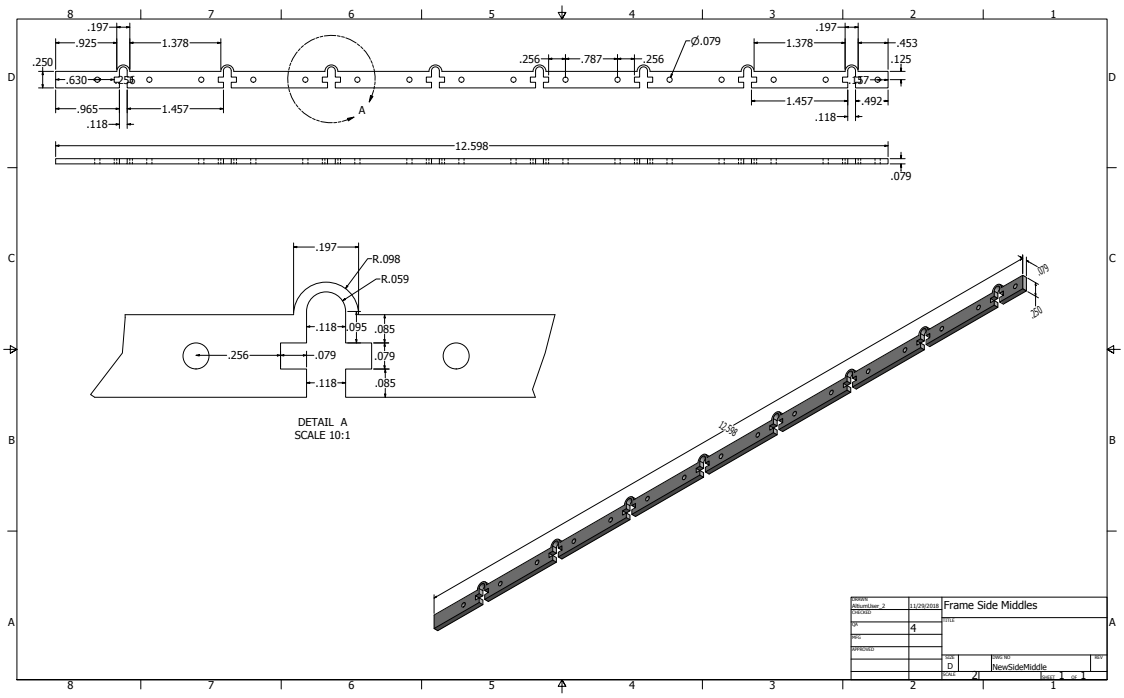

Figure 11: Design of longer middle sections of 2 mm thick inner side frames using PEEK for low-mass detector.

Alexander Kiselev on the implementation of a forward tracker simulation based on Triple-GEMs. Working with a second undergraduate back at FIT, he succeeded in installing EicRoot in a Docker environment as well as directly in a CENTOS7 environment.

For a first study, he compared the momentum resolution of tracks measured with three GEM chambers with three standard copper foils each vs. those with the equivalent of two chromium foils and one standard foil each. A 3-1-2-1 mm GEM gap configuration and a beam of 1 GeV/c electrons emitted from the IP at 25° to the beam line are used. The geometry of this study and an example track are shown in Fig. 12.

The first configuration comprises three standard GEM foils, i.e. 5 μm thick planes of copper on both sides of a 50 μm thick plane of polyimide material. The distribution of the differences between reconstructed momentum and MC-truth momentum for this configuration has a Gaussian shape with a root mean square of 7.7% (Figure 13(left)). For the configuration with chromium GEM foils, a 50 μm thick plane of polyimide should be sandwiched between two planes of 200 nm thick planes of chromium. Since no direct method of using chromium foils is possible in EicRoot, the thickness of copper that would be equivalent to two foils with 200 nm of chromium and one of 5 μm of copper is plugged into the variable defining the thickness of copper in the GEM foils. In effect, this reduces the amount of copper by a factor three. The Gaussian fit for this chromium GEM configuration has an associated root mean square of 7.5%. Comparing the RMS values for standard and chromium GEMs, one can see that they differ by only 0.2% in favor of the chromium configuration. This implies that reducing the material from copper to chromium in two of the GEM foils has a minimal impact on the momentum resolution for this scenario.

R&D on μRWELL detector: We received a $10\times10\,\mathrm{cm}^2$ resistive micro-well detector (μRWELL) from CERN in late September and began some basic R&D on this detector technology for the purpose of fast tracking in the barrel region of the EIC detector. To complement the 2D readout with Cartesian strips chosen by the UVa group for their μRWELL detector prototype, we opted for a 1D zigzag strip readout foil

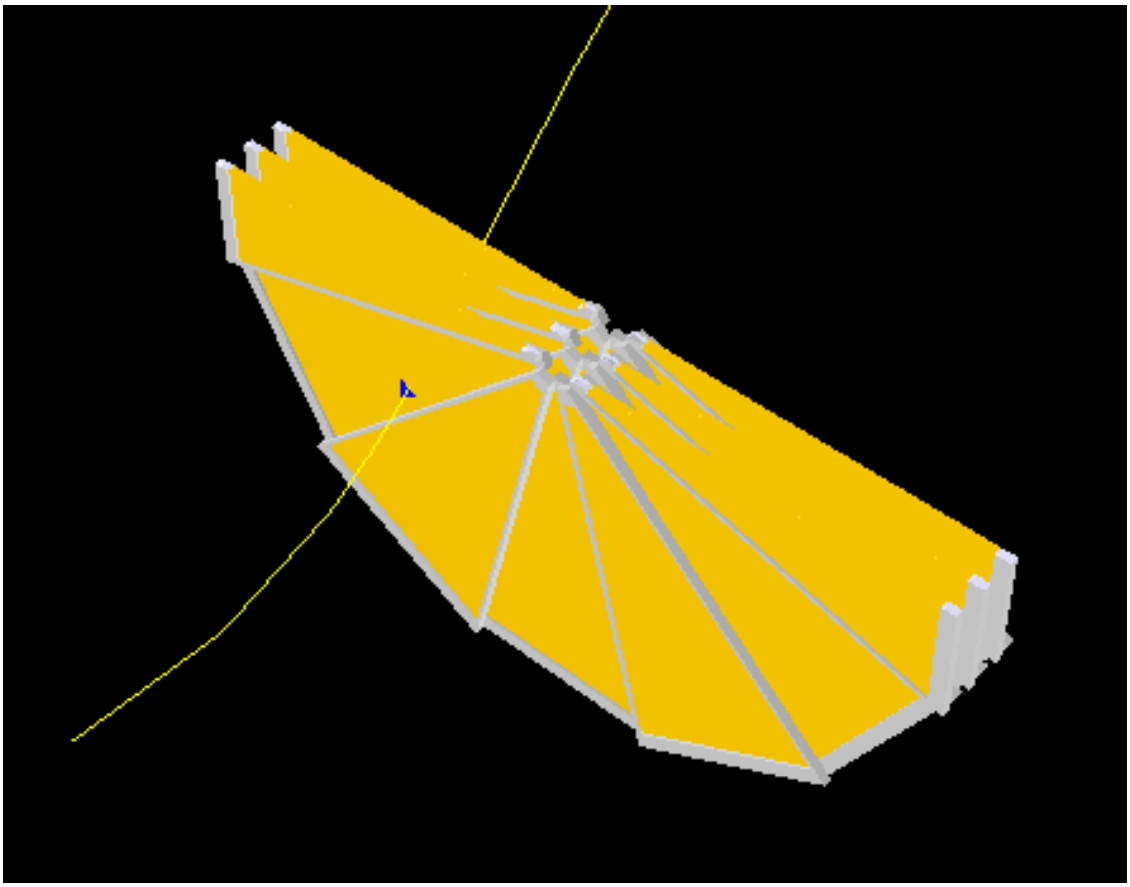

Figure 12: EicRoot simulation of a 1 GeV/c electron track reconstructed in three GEM stations in forward tracker region.

based on the foil design that we had used for the $10\times10\,\mathrm{cm}^2$ GEM prototype[5] of the low-mass FT detector. This readout is mounted on a honeycomb structure for additional mechanical support.

In their last report the reviewers had recommended to test the basic viability of a cylindrical detector design with a simple polyimide foil. As it turned out, an issue had arisen with the manufacturing of our first μRWELL foil at CERN that resulted in a larger outer diameter of the wells on this μRWELL foil - approximately 80 microns instead of the nominal 70 microns. As a larger diameter would compromise the gain performance, this foil could not be used in a detector. Keeping the reviewer's recommendation in mind, we requested that CERN send us this problematic unmounted foil for some basic investigations related to curving a μRWELL foil before shipping the full detector kit with a proper μRWELL foil.

A microscope calibration slide was used to measure the outer diameter of several wells on the compromised foil under a microscope, and a mean value of 81.2 ± 1.7 microns was obtained confirming the issue detected at CERN. We also measured the thickness of this problematic foil to be $0.180 \pm 0.007\,\mathrm{mm}$. The foil was then placed in a mount and bent in convex and concave orientations (Figs. 14a and 14b) with radii down to about one inch and observed under a microscope (Fig. 14c). There did not appear to be any obvious disfiguration, such as a delamination or a change in the shape of the micro-wells, as a result of the bending.

The contents of the actual μRWELL detector kit were also first closely inspected upon arrival. Measurements were taken again with the microscope calibration slide in order to determine the diameters of the wells at the bottom (inner diameter) and at the surface of the foil (outer diameter). The measurements shown in Tab. 1 confirmed the proper geometry of this second μRWELL foil. A conductive grounding ring is placed on the

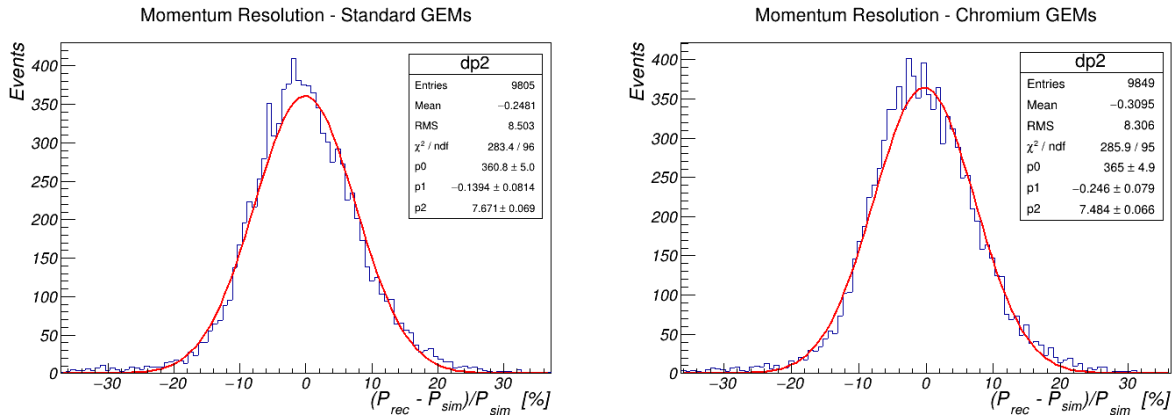

Figure 13: Momentum resolutions for 1 GeV/c tracks measured with three rings of forward tracker GEMs in EicRoot simulation. Left: Standard GEMs with copper foils. Right: GEMs with 2 chromium foils and 1 copper foil.

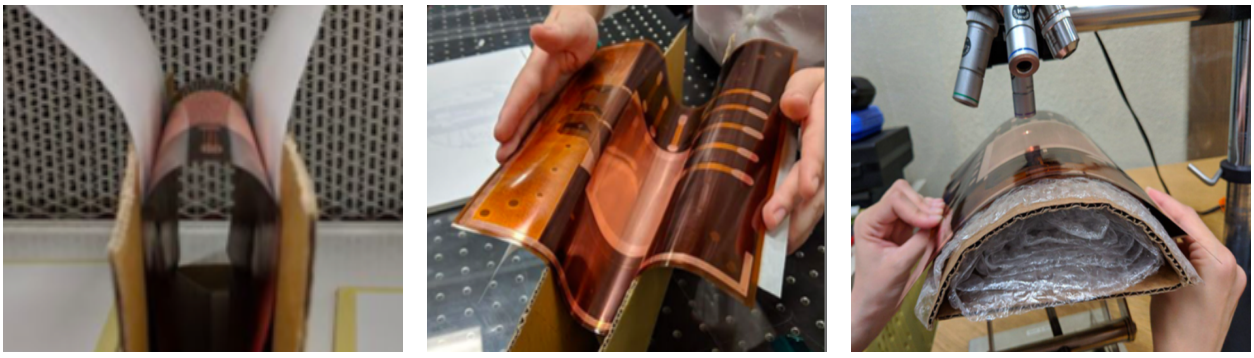

(a) Convex bending. (b) Concave bending. (c) Bent foil under microscope.

Figure 14: Bending tests with an unmounted μRWELL foil.

DLC and surrounds the active area. It allows the sinking of charge produced in the wells. Some tarnish was visible on the active region (Fig. 15a), which was then investigated under the microscope. In the process, a texture constituting small "bumps" or "divets" was observed at the bottom of the wells (Fig. 15b), which did not appear to be correlated with the tarnish on the surface.

Table 1: Mean Measured Well Diameters.

Inner Diameter	$(38.9 \pm 2.7)\mu m$
Outer Diameter	$(70.0 \pm 3.5)\mu m$

We hypothesized that this texture was a feature of the DLC, and an investigation was conducted to determine if the DLC could be accessed from a location other than the base of the wells. As seen in Fig. 16a, the layer of dark DLC material extends beyond the active region of the board and the grounding ring. When viewed under the microscope, that material, shown in Fig. 16b, possesses the same bumpy texture seen in the base of the wells. If this was an exposed area of the DLC, one would also be able to measure its resistivity. One report had indicated to expect a resistivity of 12 MΩ per square for such a $10\times10\,\mathrm{cm}^2$ DLC layer. We attempted to measure the resistivity of the DLC layer directly. However, testing with a Megger insulation meter across a small distance in this marginal region yielded a resistance over 20 GΩ. Ultimately,

confirmation was received from CERN that due to the manufacturing process the DLC layer is actually completely covered with polyimide including in the exposed margins, and therefore it is not accessible for direct resistance measurements. However, CERN indicated that this will be modified in future μRWELL detector kits so that DLC resistivities can be checked directly.

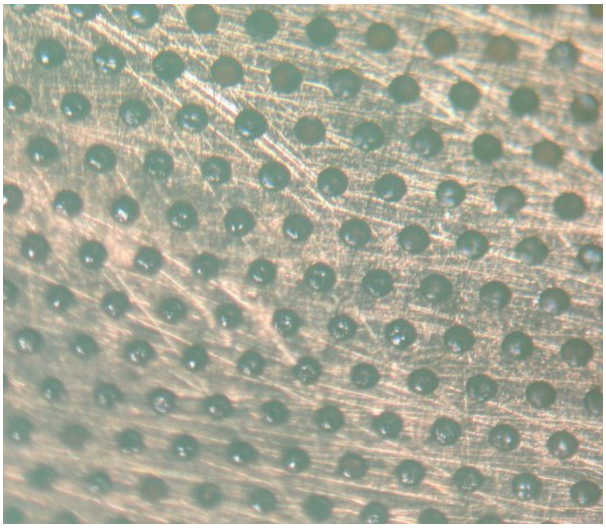

(a) The tarnished area of conical wells in the μRWELL foil.

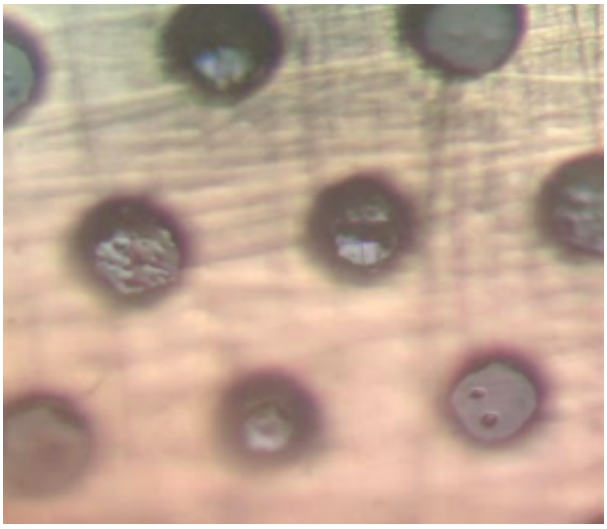

(b) Texture visible at the bottom of the wells under higher magnification.

Figure 15: Images of the μRWELL structure taken under a microscope.

(a) Dark material extending beyond active region and grounding ring.

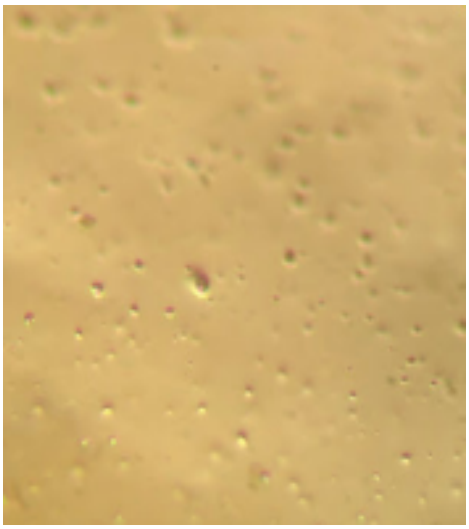

(b) Bubbles or divets seen on this dark material under higher magnification.

Figure 16: Microscope images of the dark DLC material at the margin of the active area.

After the stack and outer frame preparations were complete, the detector was completed by installing the polyimide window and lid and sealing with the closing screws (Fig. 17). Caution was taken to clean all components of the detector, especially the active region, before closing the detector in order to prevent any particulate contamination that could cause sparking.

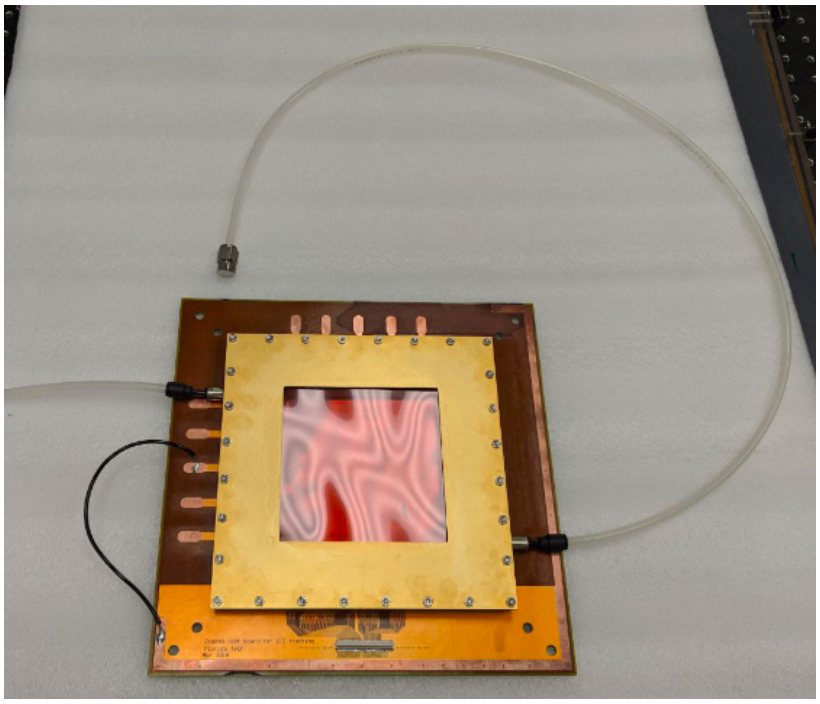

Figure 17: The μRWELL detector assembled and attached to gas lines. The DLC grounding ring is connected with a black wire to the PCB ground. At the bottom a Panasonic connector provides the connection to the zigzag signal strips.

2.3.3 INFN Trieste

Activity in period July 2018 - December 2018

1. **Test beam studies of a prototype of the single photon detector by MPGD technologies with miniaturized pad-size**
   The prototype architecture consists in two staggered THGEM layers, the first one also acting as photocathode substrate, followed by a resistive MM by discrete elements. The detector active surface is 100×100 mm^2. The THGEM geometrical parameters are: 400 μm hole diameter, 800 μm pitch, 400 μm thickness and hole without a rim. The MM has 128 μm gap; the pad-size is 3×3 mm^2 with 3.5 mm pitch, forming a matrix of 32×32 pads (in total 1024 pads). The pads are grouped in 32×4 modular units; each unit is equipped with a connector interfacing the signal pads to the front-end electronics and a second, identical connector, providing the biasing voltage to the anode pads via protection resistors, one per pad, housed in a dedicated resistor board. Figure 18 illustrates the detector design. The prototype has been built and fully tested in laboratory, as reported in July 2019. The main exercise of the present reporting period concerns the test beam studies of the prototype performed at CERN over two weeks between the end of October and the beginning of November 2018. During the test-beam period, we have been main-users for part of the time and otherwise we have worked in parasitic mode. High energy (>100 GeV) muons or pions have been alternatively delivered.

   A compact test-beam setup was prepared, assembled and equipped in Trieste (Fig. 19). It includes:

   - The mechanical support of the detectors; it houses also the HV and LV power supplies.
   - The system of scintillation counters that form the trigger: four finger-shaped counters are used in coincidence, two placed upstream of the prototype and two downstream of it; in both couples, the detectors are arrange with orthogonal orientation, so to define a cross with a small overlap

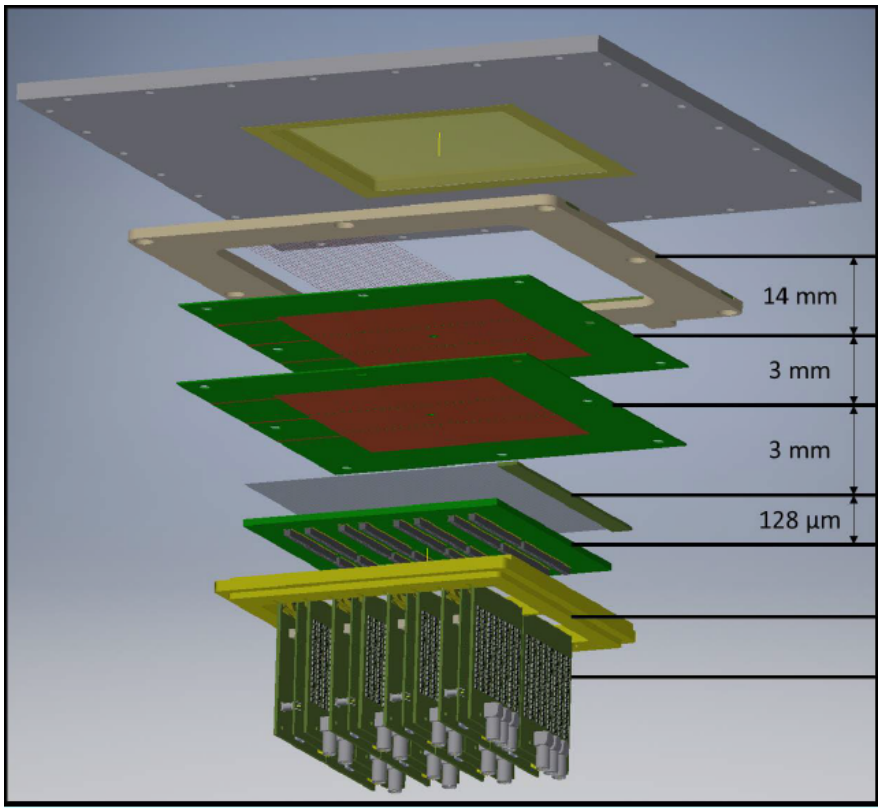

Figure 18: Exploded view drawing of the prototype.

surface of 3×3 mm^2 for the first couple and 5×5 mm^2 for the second one. The purpose of this arrangement is to select beam particles crossing the detector almost perpendicularly at a well-defined location; the position of the finger-shaped counters is remotely controlled by step motors to facilitate the alignment.

- The prototype detector with its read-out electronics.
- A fused silica radiator is mounted onto the prototype; it has cylindrical symmetry and a dedicated design: the majority of the Cherenkov photons generated by minimum ionizing particles with trajectories quasi-parallel to its axis hit the detector surface in a ring-shaped area (Figs. 20, 21). A shutter is situated between the radiator and the photocathode and it is remotely controlled via a piezoelectric actuator.
- The read-out system is based on the SRS/APV25 system [39] developed within the RD51 collaboration. The 1024 pads are read-out by eight APV25 chips, 128 channel each. The chip control and the DAQ is ensured by the novel DAQ Raven system, entirely LabView based, developed within our R&D activity in order to ensure large acquisition band width. The Raven system architecture and performance have been reported about in January 2018. Dedicated interface boards have been designed and realized to interface the detector connectors and the SRS/APV25 FE boards.

The last phase of the detector assembly consists in inserting in the detector the THGEM coated with the CsI film, that must not be expose to air in order to preserve its quantum efficiency. This implies that the final assembly is performed in a glove-box (Fig. 22), including mounting the fused silica radiator and the shutter. A picture of the prototype fully equipped and installed at the test-beam is shown in Fig. 23.

Data have been collected using two different gas mixture, namely (a) Ar:CH_4 = 50:50 and (b) pure methane, and different voltage settings in order to determine the optimal operation conditions. The data analysis has just started and in the following we provide some preliminary information obtained

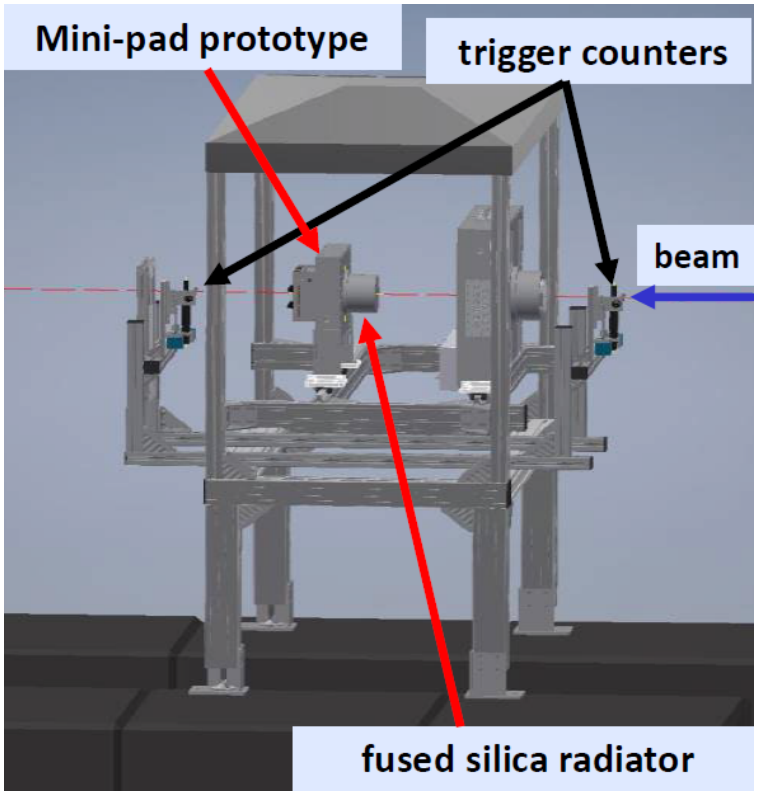

Figure 19: Sketch of the test-beam set-up.

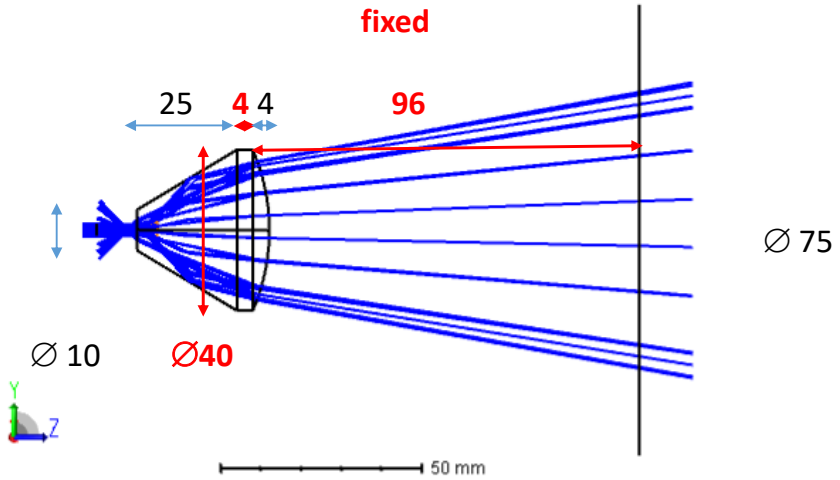

Figure 20: Cross-section of the fused silica radiator with cylindrical symmetry. The blue lines are examples of Cherenkov photon trajectories; a large fraction of them intercepts the photocathode surface (the vertical black line in the drawing) in a ring-shaped region, even if some of the photons hit the photocathode in different areas. The majority of the photons generated in the radiator are trapped inside the radiator itself due to total reflection; there are no examples of these trajectories in the drawing.

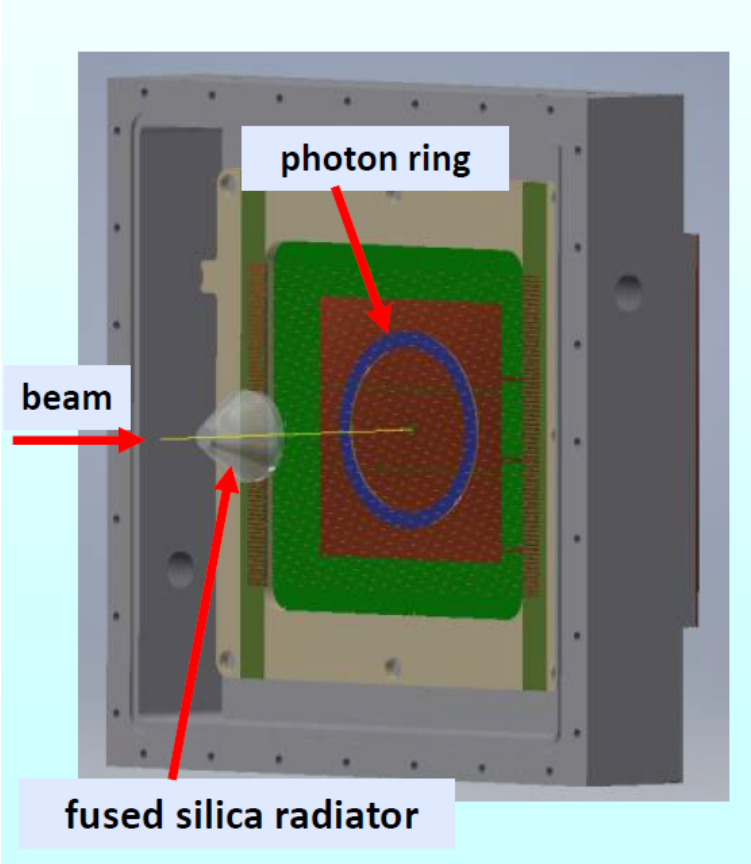

Figure 21: Skematic drawing illustrating the formation of the ring image in the photon detector by Cherenkov photons generated in the fused silica radiator.

from the data collected with gas mixture (a) and with the muon beam. It is relevant to underline that, aiming at single photoelectron detection, we have to deal with an exponential amplitude spectrum, where the majority of the population is at small amplitudes. Therefore, we have to apply to the signals small threshold-values and a good control of the noise is important. At present, in the data analysis, we have not yet implemented the subtraction of the common-mode noise and, therefore, the following preliminary plots are still affected by non-negligible noise contributions. In this preliminary analysis, the software threshold applied to the amplitude is at the level of 4.5$\times$ the noise r.m.s. . For each event and for each read-out channel, 27 consecutive amplitude measurements are registered. The time distance between two consecutive measurements is 25 ns. The time development of a typical signal is shown in Fig. 24: the 27 consecutive measurements of the signal amplitude in all the 128 channels of an APV25 chip are shown. A signal is present in one of the channels. The plot has ben obtained on-line using one of the features of the Raven DAQ system. In the following, the time respect to the trigger associated to the heighest amplitude of a channel is used: the resulting time distribution of the signals with amplitude above threshold is shown in Fig. 25. A clean peak is visible fully contained in bins: 6-10, namely in a 125 ns time interval; in the following a corresponding time-cut is applied.

The 2-D histogram of the hits for a sample of events collected with the shutter between the radiator and the photocathode open is shown in Fig. 26. A ring is clearly visible as well as, at the center of the ring, the hits due to the minimum ionizing particles crossing the detector. In a corresponding histogram for data collected with the shutter closed (Fig. 27) the ring is no longer visible, while the particle signal is still present. Subtracting the second histogram from the first one applying proper normalization with the ration of the number of events in the two samples, the particle signal disappears, while the ring

Figure 22: Pictures illustrating the final phase of the prototype assembly, which is performed in a glove-box.

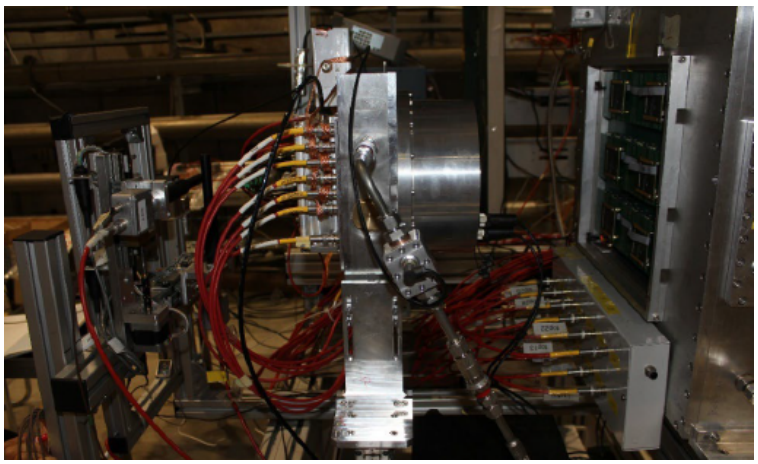

Figure 23: Picture of the fully-equipped prototype installed at the test-beam.

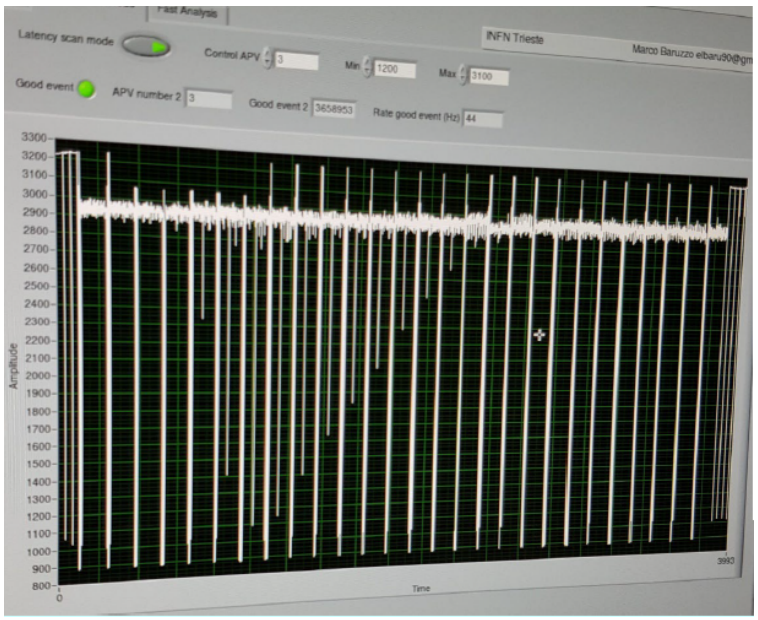

Figure 24: 27 consecutive measurements of the signal amplitude in all the 128 channels of an APV25 chip are shown; the time interval between two consecutive measurements is 25 ns. The development of a physical signal versus time can be seen in one of the APV25 channels.

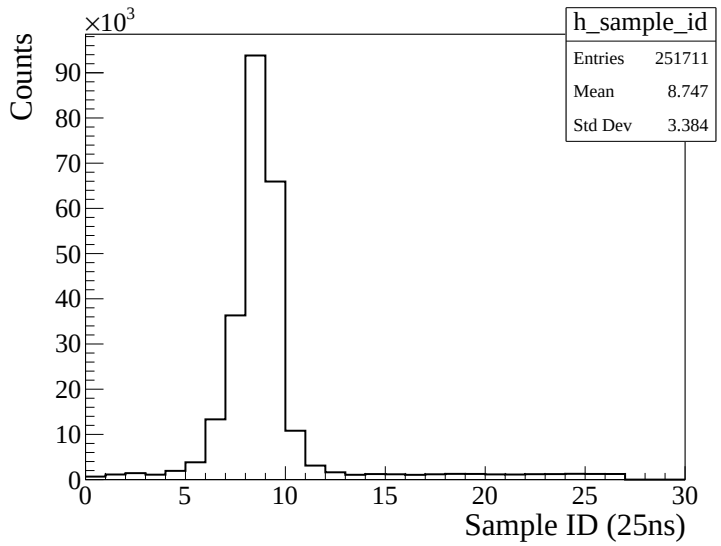

Figure 25: Time distribution of the signals respect to the trigger time.

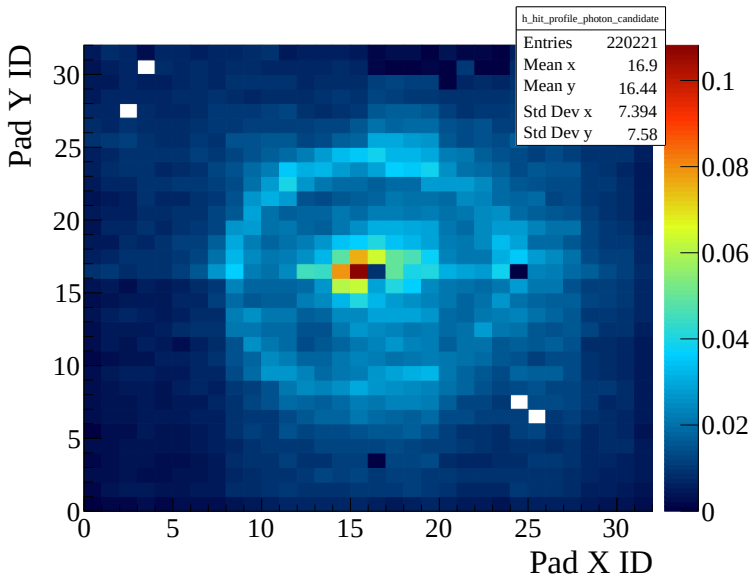

Figure 26: 2-D histogram of the hits for a sample of events collected with the shutter between the radiator and the photocathode open.

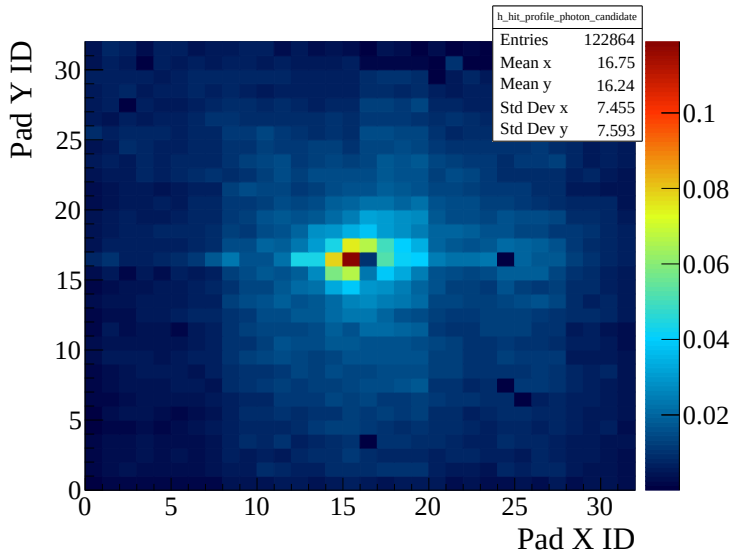

Figure 27: 2-D histogram of the hits for a sample of events collected with the shutter between the radiator and the photocathode closed.

is clearly visible and, outside the ring-region, the population in the histogram bins fluctuates around zero. (Fig. 28). Therefore, it can be concluded that Cherenkov photons are clearly detected.

A preliminary algorithm performing hit clusterization is applied to the hits in the ring area. The distribution of the cluster amplitude is used to extract information about the detector gain, as shown in Fig. 29: the resulting gain has the remarkable value of 50k.

The analysis of the test-beam data is in a very initial stage and has to be continued and improved in the coming months. Nevertheless, the first indications are very positive: the prototype has successfully

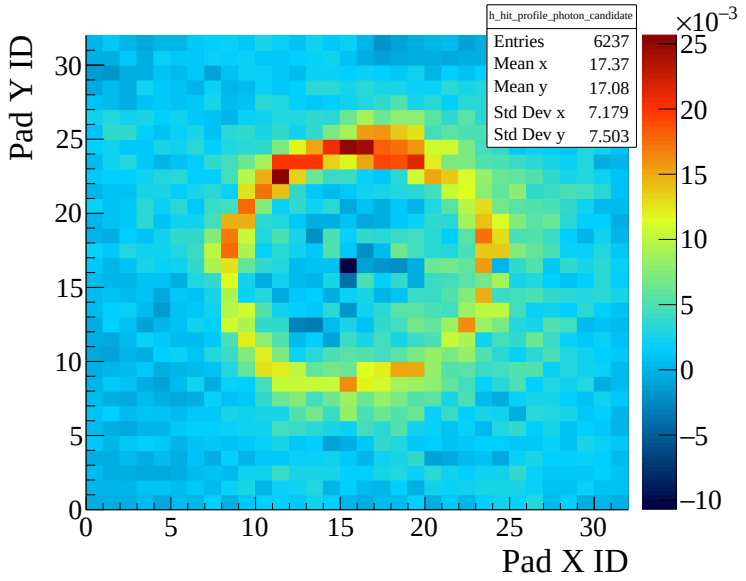

Figure 28: 2-D histogram of the difference between the 2-D histograms for events collected with the shutter between the radiator and the photocathode open and closed. The histogram population has been normalized with the ratio of the number of events in the two samples.

detected single photons and it has been operated at large gain.

2. Initial studies to understand the compatibility of an **innovative photocathode based on NanoDiamond (ND) particles** with the operation in gaseous detectors and, in particular, in MPGD-based photon detectors
   The results of the characterization of the first THGEMs coated with ND powder have been reported in July 2018. An aspect is surprising and puzzling: the THGEMs with ND powder coating exhibit higher gain for a given biasing voltage respect to the gain measured for the same THGEM before applying the coating. The characterization measurements have been repeated, confirming the result, while a possible explanation is emerging. The coating layer is resistive and it covers both the metallized part and insulating part of the THGEM. Therefore, its presence can prevent the charging up of the insulating surfaces. It is expected that the THGEM multiplication is higher when there is no charging up. This hypothesis has to be supported by further measurements.

   In parallel, in order to prepare further studies, actions towards material procurement are taking place, both concerning new ND powder samples and more small-size THGEMs.

Concerning the **dissemination of the results**:

- The initial results concerning the performance of the photon detector prototype with miniaturized pads have been present at **the 14th Pisa Meeting on Advanced Detectors**, La Biodola, Isola d'Elba (Italy), 27 May - 02 June 2018, [40] and at **the 10th International Workshop on Ring Imaging Cherenkov Detectors**, Moscow (Russia) 29 July – 4 August 2018.
- The first studies concerning the coupling of ND photocathodes and MPGDs have been presented at **the 10th International Workshop on Ring Imaging Cherenkov Detectors**, Moscow (Russia) 29 July – 4 August 2018[41]

Concerning the **milestones for 2018**:

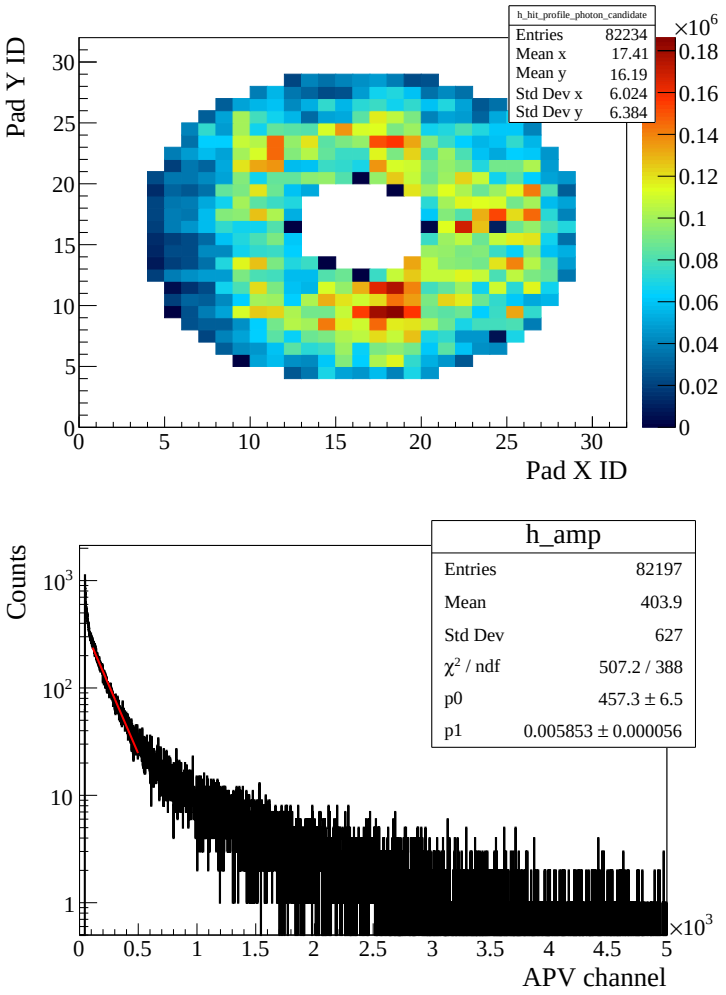

Figure 29: Events collected with the shutter between the radiator and the photocathode open. top) 2-D histogram indicating the ring area. bottom) Amplitude spectrum of the reconstructed clusters in the ring area; the spectrum is fitted to an exponential function, where the inverse of the slope represents the mean amplitude in ADC channels.

- **September 2018: The completion of the laboratory characterization of the photon detector with miniaturized pad-size.**
  The exercise has been completed and the milestone is successfully matched.
- **September 2018: The performance of the tests to establish the compatibility of the ND photocathodes with the operation of MPGD-based photon detectors.**
  The tests have been performed and, therefore, the milestone is partially matched. Nevertheless, there is not yet a solid answer to the question related to the compatibility: the totally unexpected results demand for further investigation in 2019.

2.3.4 Stony Brook University

Ion Back Flow A TPC prototype has been constructed and a sophisticated test-beam setup established. We purchased picoammeter from PicoLogic in Zagreb/Croatia which is a unique device that allows to measure

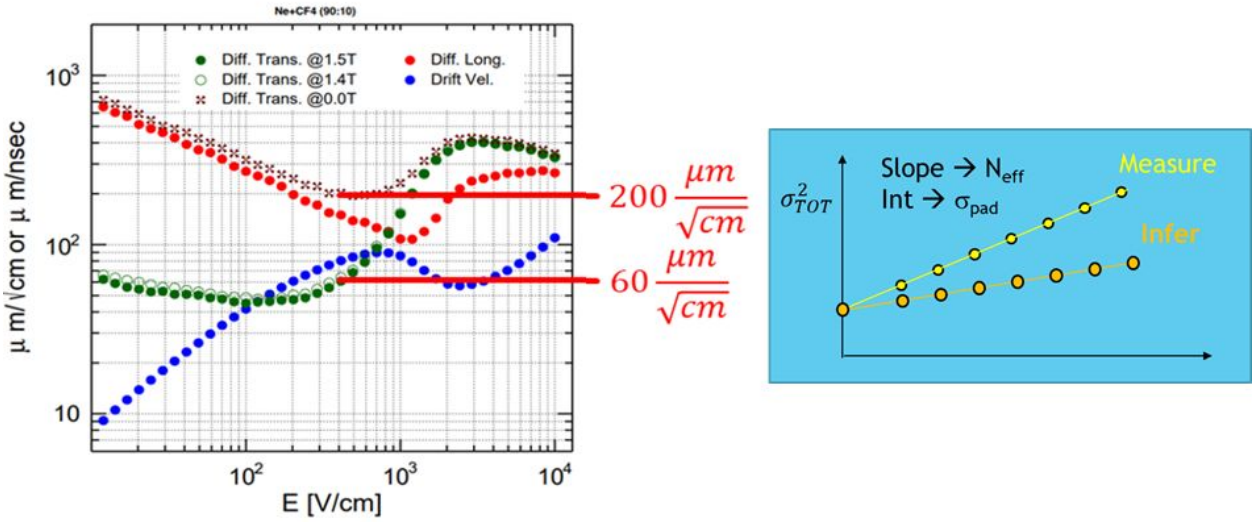

Figure 30: Principle for the determination of space point resolution at B = 0 T and extrapolation to B = 1.4 T.

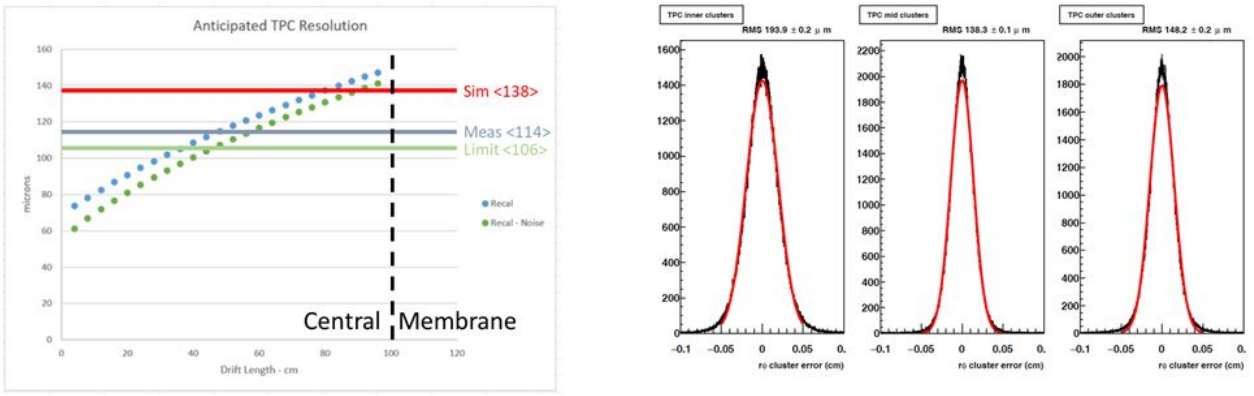

Figure 31: Comparison of measured (left) and simulated (right) space point resolution.

very small currents at high potential. The floating current measurements can be performed at potentials much larger than 5 kV, ideally suited for IBF measurements in a TPC.

The TPC prototype has been equipped with a real size readout module, based on a quadruple-GEM stack similar to the ALICE-TPC readout and zig-zag pad readout structure. The prototype has been exposed to the 120 GeV protons at the Fermilab Test Beam Facility (FTBF) to establish the working parameters of the TPC. We have analyzed the data obtained from the test-beam campaign and verified the performance parameters of the prototype. The resolution has been obtained by measuring with a drift-length of 40 cm at B = 0 T and extrapolated to the magnetic field with the Babar magnet at B = 1.4 T by means of

$$\sigma^2_{total} = \sigma^2_{int} + \frac{D^2_T L}{N_{eff}} + \sigma^2_{sc}\,,$$

with $\sigma_{int} = \sigma(z = 0)$: intrinsic resolution, D_T: diffusion constant, L: drift length, N_{eff}: effective number of electrons leading to the readout signal and σ_{sc}: smearing due to space charge distortions. The smearing due to space charge distortions can be neglected at the test-beam. The measurement/extrapolation principle can be taken from Fig. 30. The results for this procedure are shown in Fig. 31.

Mirror coating We have continued to install components of the electron-/ion-gun for the evaporation of thin layer structures on mirror surfaces. The installation is running smoothly and undergraduate students are gaining experience in handling the sensitive equipment under the supervision of senior personnel. The installation process also helps in understanding the equipment and in preparing the start-up procedure of operation.

Meta-materials We have started evaluating procedures of transformation optics with which one can obtain properties of materials that allow to modify the Cherenkov angles but maintaining the momentum reach for high momentum particles. Based on the dispersion relation (from [42])

$$\frac{k_x^2}{f'^2(x)} + \frac{k_y^2}{g'^2(y)} + \frac{k_z^2}{h'^2(z)} = \epsilon_b \frac{\omega^2}{c^2}$$

and substituting $f'(x) = F\ (= \frac{\partial x}{\partial x'})$, $g'(y) = G\ (= \frac{\partial y}{\partial y'})$, $h'(z) = H\ (= \frac{\partial z}{\partial z'})$ we were able to reproduce the simulated results obtained in [42], Figs. 1 a) and b). These reproduced results can be seen in Figs. 32, 33.

2.3.5 Temple University

Commercial Triple-GEM Detectors

Temple University was able to achieve several goals that were set for this funding cycle. Last summer two commercial triple-GEM detectors were built, one using Kapton rings as the spacers between the GEM layers and another using more traditional G10 spacer grids. Upon completion of the two triple-GEM detectors, they were inserted into the cosmic ray test bench where both detectors drew about twice as much current as the STAR FGT triple-GEM detectors, and exhibited excessive sparking. This sparking ultimately led to both detectors failing and becoming unusable. After opening the detectors and inspecting the layers, the effects of excessive sparking were clear, as can be seen in fig. 34. It was hypothesized that the sparking was a result of shorts originating in the HV connector pads on the GEM foils in each layer. Each GEM foil is segmented into nine HV sectors on one side, while the other side is unsegmented. Each of the nine HV sectors connects to three HV pads located at the top of the GEM foil. Additionally, there are three pads which connect to the unsegmented side of the GEM foil, as shown in fig. 35. The HV pin connections are then made to a HV pad position that is associated with one of the three triple-GEM layers, *e.g.* the middle GEM foil layer has HV pins connected to the HV pads in the center of the three pads for each sector. In the initial two triple-GEM detectors built, the unused HV pads for each GEM foil layer were left in tack with the thinking that the pins passing through the unused HV pads would be isolated from them since they are not physically touching the HV pads. However this turned out not to be the case and was found to be the cause of the shorts in the initial commercial triple-GEM detectors. This was verified during the building of the third commercial triple-GEM detector. After stretching and gluing all foils to their respective frames, the triple-GEM stack was assembled by simply stacking the various layers without glue. We then tested the detector for shorts amongst the HV pins, where we were able to generate shorts with minor movements of the HV pins. The stack was then disassembled and all unused HV pads on each GEM foil were cut away. The detector stack was reassembled and tested again for shorts. With the excess HV pads removed we were not able to detect any shorts. Gluing the stack of the third commercial GEM detector and inserting it into the cosmic ray stand, we now see the same current being pulled as that STAR FGT triple-GEM detectors pull. This suggests that the shorting issue that plagued the first two triple-GEM detectors is now solved.

Now that the shorting issue has been resolved we are ready to begin the characterization of the triple-GEM detector. Figure 36 shows some initial reconstructed cosmic ray hits. While verification of a signal in the prototype is great, one would expect a more uniform distribution of the cosmic ray events. There could be several factors which are contributing to the non-uniform event reconstruction. First it was noticed during leakage current testing that one GEM layer displayed relatively high leakage current. Secondly, during pedestal checking of the detector two APV chips were found to be dead. Furthermore inefficiency could also

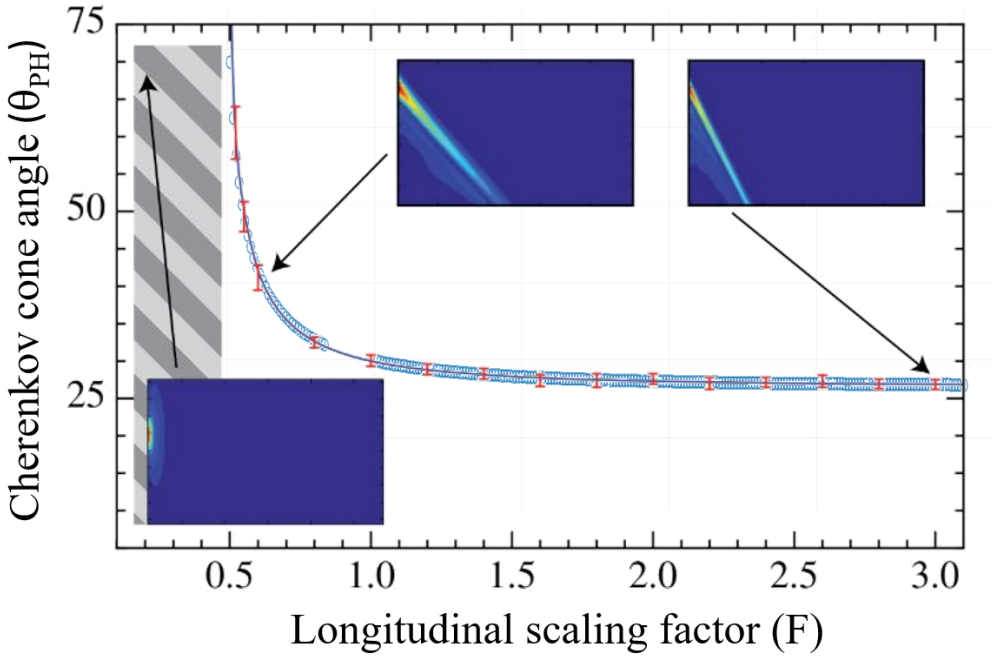

Figure 32: Data reproduction (open blue circles) based on the calculations obtained from the transformation optics overlaid on [42] Fig. 1a).

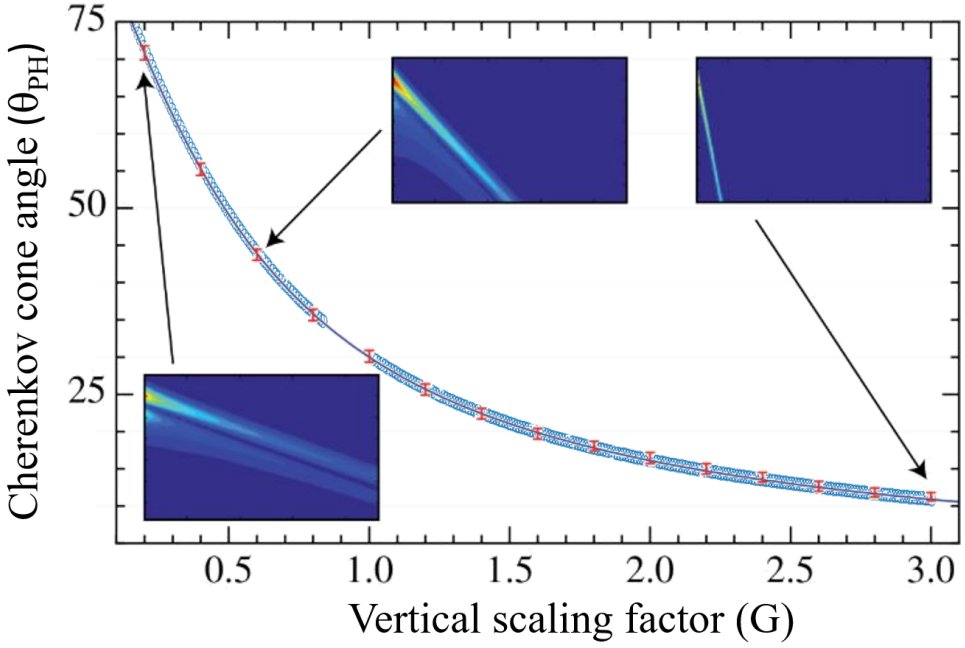

Figure 33: Data reproduction (open blue circles) based on the calculations obtained from the transformation optics overlaid on [42] Fig. 1b).

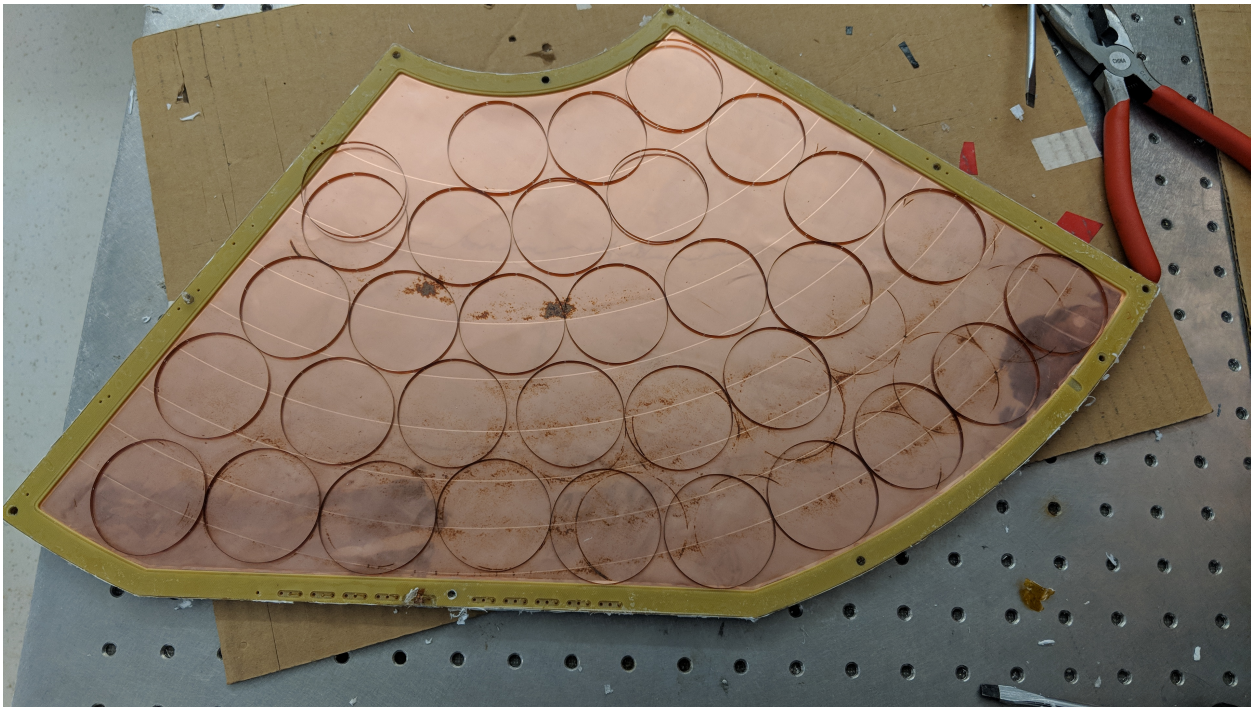

Figure 34: Damage to a GEM layer in the first commercial triple-GEM detector caused by excessive sparking resulting from electrical shorts.

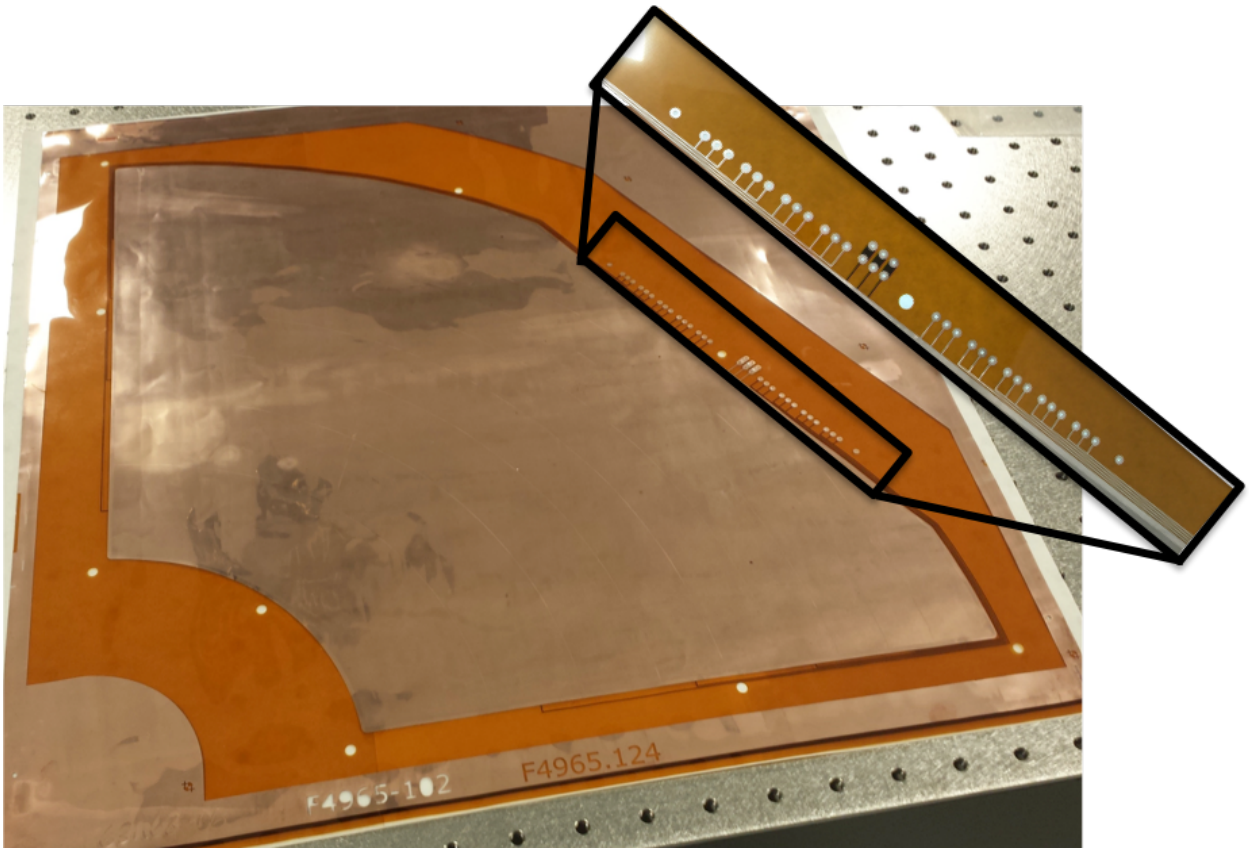

Figure 35: Commercial GEM foil HV sectors and connection pads.

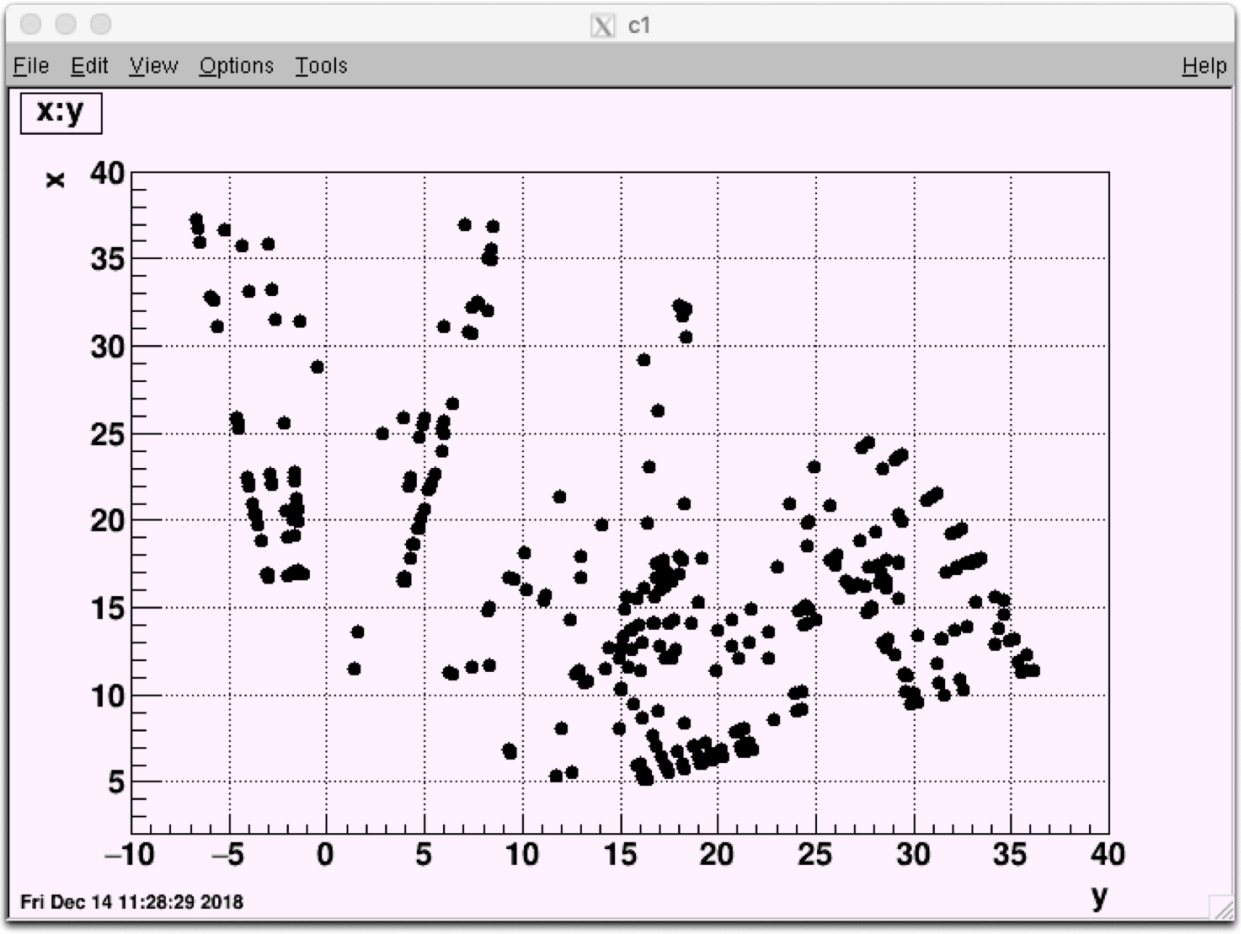

Figure 36: Third commercial triple-GEM detector showing reconstructed X-Y hits of cosmic ray events.

be due to the fact that we have not yet tuned and optimized the APVs since we first wanted to verify the detection of a signal in the detector. Finally, more data will be needed to better understand the effect that the Kapton rings have on generating dead area within the detector. Further characterization and investigation is underway. There is enough material remaining to assemble a fourth commercial triple-GEM detector. The GEM, readout, and HV foils for this detector have now been stretched and glued to their respective frames. The assembly of the GEM stack was delayed until we saw how the third triple-GEM detector performed, in case we needed to correct any unforeseen issues.

MPGD μTPC Simulation

In addition to the hardware work, we are also working on some simulations. The initial machinery needed to produce a MPGD detector in μTPC mode has now been implemented. This machinery allows one to create a barrel geometry with a specified dead material radiation length and drift gap filled with a particular gas. This machinery also allows one to simulate multiple hit points by defining sensitive barrel layers within the drift gap volume. The resolution parameters of the detector are also adjustable. For example one can specify the detectors radial and transverse resolutions, as well as its hit point resolution. This machinery has now been tested using some nominal settings and is currently being modified to reflect more realistic parameters and digitization.

2.3.6 University of Virginia

Large EIC GEM prototype with 2D U-V strip readout

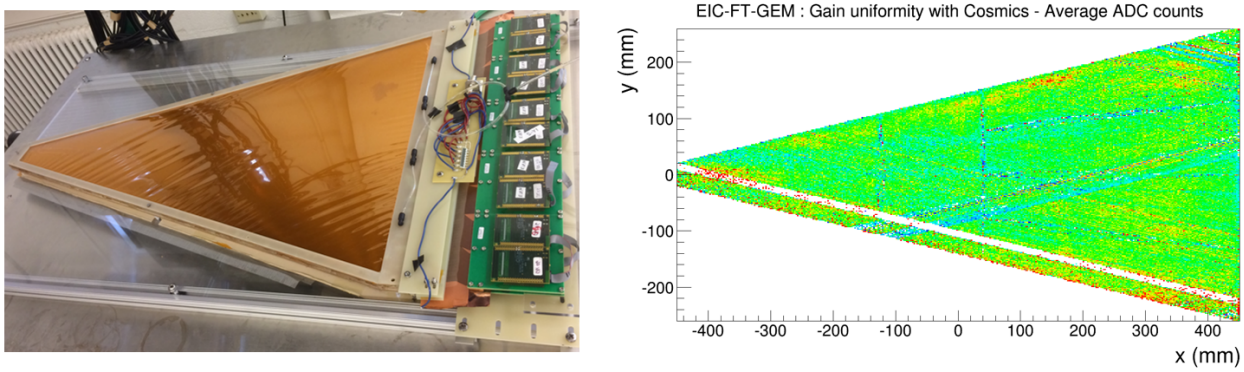

Figure 37: (*Left:*) large EIC GEM prototype on the cosmic bench at UVa; (*right:*) Gain uniformity: Distribution of the average charge in ADC counts.

Characterization with Cosmics: Preliminary tests of the large EIC GEM prototype with cosmics showed a gain about an order of magnitude lower than the expected value of 8000 of typical triple-GEM operating with Ar-CO2 (70/30) mixture at the nominal voltage 4.1 kV. A likely explanation of the lower gain may be that the GEM hole geometry for the GEM foil production batch, differs slightly from typical bi-conical (70-50-70 μm) shape and size of a standard GEM foil. In this case, even a relatively modest gain drop per GEM foil results to a significant drop of the effective gain in a triple-GEM detector. Increasing the voltage on the divider from 4.1 kV to 4.3 kV was enough to restore the nominal gain. However, due the large size of our prototype, we experienced various challenges related to the stretching of the GEM foils during the assembly that makes the detector very delicate to operate in a stable way at 4.3 kV or more. We therefore decided to operate the prototype with Ar-CO2 (80/20) mixture instead of Ar-CO2 (70/30), which allow us to reach a gain of $\sim 10^4$ at 4.1 kV. The prototype was characterized with cosmics for a three weeks period during which we collected about 4 million triggered events. Fig. 37 (*top left*) shows the detector on the cosmic stand in the Detector Lab at UVa. On the plot on *(top right)*, one can see a fairly uniform distribution of the average ADC (ratio of the total accumulated charge over the number of hits per unit area) across the detector's active area from cosmic data. The average ADC distribution plot is a measure of the gain uniformity in the GEM chamber. Efficiency drop caused by the presence of GEM support spacers are visible on the plot as well as dead areas due to a few broken strips or missing contact between the strips and the FE electronics. The overall uniform detector response, successfully demonstrates that the double-sided zebra connection technique that we developed for the readout electronics works as expected. The analysis of the cosmic data is still ongoing.

Characterization of large EIC GEM prototype at Fermilab beam test: The large EIC GEM prototype, together with two small $10\,cm \times 10cm$ prototypes, the μRWELL detector with X-Y straight strips readout and a triple-GEM with 2D zigzag strips, were brought to the Fermilab Test Beam Facility (FTBF) this summer (June - July 2018) to study the spatial resolution performances with the 120 GeV primary proton beam. Our eRD6 colleagues from BNL provided four small triple-GEM with COMPASS 2D X-Y readout for the tracking. The setup is shown on Fig. 38 with the large EIC GEM on the moving X-Y moving table of the MT6.2b area and the BNL GEM trackers as well as the μRWELL prototype used in the upstream and downstream telescopes. The detector configuration for this setup was optimized to minimize the multiple scattering impact on the resolution studies. All detectors operated with the same Ar-CO2 gas mixture (70/30) and were read out using the APV25-based Scalable Readout System (SRS) electronics developed at CERN by the RD51 collaboration. For the DAQ, we used DATE and AMORE

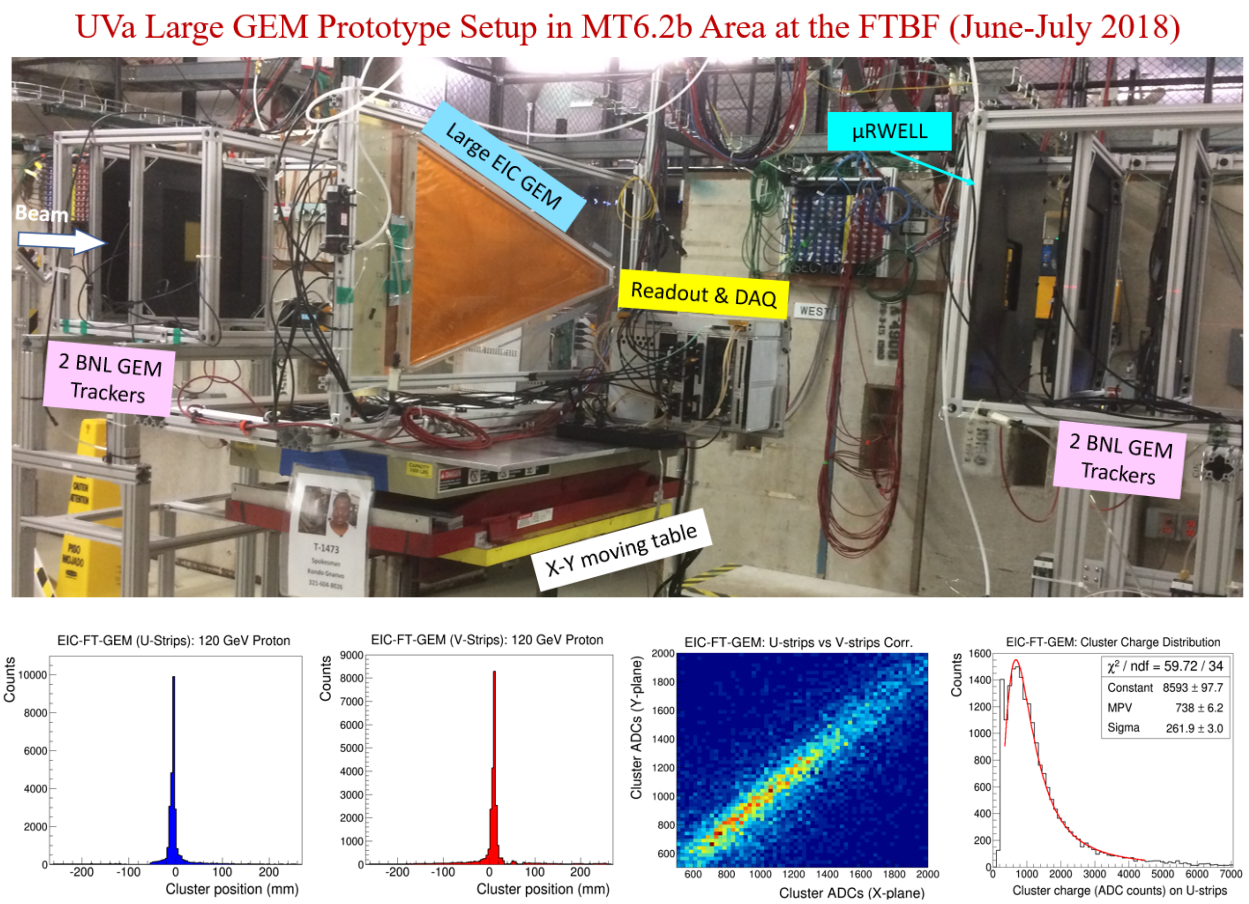

Figure 38: *Top:* Large GEM setup at FNAL FTBF with two BNL GEMs for the upstream telescope and two other and the small μRWELL prototype for the downstream telescope. *Bottom:* Characteristics of the prototype; *Left to right:* 120 GeV proton beam profile on U-strips and V-strips; Charge sharing correlation between the top (U-strips) and bottom (V-strips); Charge distribution in ADC counts on U-strips.

software, developed by the CERN ALICE experiment and the system was triggered by scintillators/PMTs coincidence signal provided by the facility at a trigger rate of $\sim$ 500Hz.
The plots on the left of Fig. 38 show the 120 GeV proton beam profile reconstructed respectively on the top (U-strips) and bottom layers (V-strips) of the U-V strips readout foil. Plot on center right shows excellent charge sharing correlation between U-strips and V-strips. The charge distribution (in ADC counts) of the top layer (U-strips) is shown on the right plot. The distribution fits nicely with the Landau function as expected from minimum ionizing particles. This new U-V strips readout foil design developed for this prototype is a clear improvement of the previous iteration tested in the first large EIC GEM prototype in 2013 [38].

Production quality issues with the U-V strips readout foil: Fig. 39 shows the 2D reconstruction of the proton beam from position scan run. A detailed analysis with a fine binning around the beam spot areas reveals some unexpected patterns of reconstructed positions as can be seen on zoomed-in area of two beam spot locations on Fig. 39. Instead of a uniform distribution of the reconstructed points, what we actually observed is a picture of the reconstructed positions heavily concentrated along a set of lines parallel to the strips. As indicated on the plots, the pattern are more pronounced ***"severe distorsions"*** in some locations than other ***"moderate distorsions"*** and suggest that a significant number of the strips may have been shorted and interconnected on both top and bottom layers during fabrication process. The effect can also be seen with the discrete set of spikes on the 1D beam profile in the U and V strips of the readout board. A

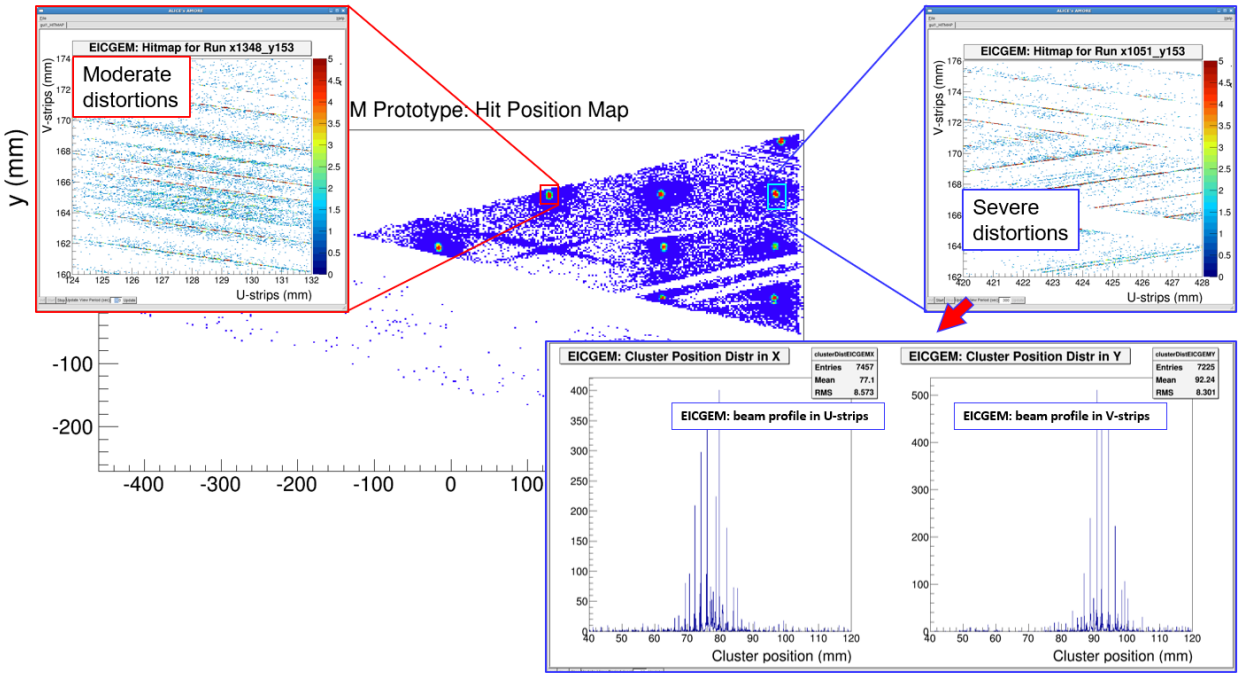

Figure 39: 2D reconstruction of 120 GeV proton beam spots from position scan run on the top active area of the prototype. A zoom in at two spots show some unexpected non uniform patterns for the distribution of the reconstructed points. These pattern can also be seen on the 1D beam profile in the U and V strips.

few consecutive shorted strips will destroy the advantage of the center of gravity method to reconstruct the position with high precision and result in the reconstructed points highly concentrated at the geometrical center of single strip causing the pattern of straight parallel lines such as the ones we observe in the plots. We can not however completely dismiss the possibility that some issues inherent to the zebra strips interface with the readout strips to the FE electronics might be the source of distorted responses at the input of the FE readout channels and degrades the position information or that a deformation of the readout board during the assembly of the detector might have results on the strange signal. The issue is under investigation.

Position residual distribution: Preliminary results on the spatial resolution of the large EIC chamber from the summer beam test are shown on Fig. 40.The plots show the position residual distribution along x and y axis of the detector at two beam spot locations. The first (top plots) in the area with moderate distortions of the reconstructed position and the second (bottom plots) in the area with severe distortions. The residual is the difference between the measured position of the proton in the large GEM and the predicted position predicted from the track obtained by a linear least square fit of the beam position in the trackers. For these results, we have not yet corrected for the track fit error nor have we accounted for the error from to multiple scattering in the detectors. But as we mentioned earlier, the setup minimizes the multiple scattering effect on the detector and we could reasonably neglect in the first order the impact of track fit error on the spatial resolution of the large GEM prototype.
For the residuals distribution in the area with moderate distortions, (top plots of Fig. 40), the width σ_y and σ_x are respectively equal to 115 μm and 426 μm. In collider environment with a cylindrical coordinate system, σ_y and σ_x would naturally translate to the spatial resolutions in respectively the azimuthal and radial direction, $\sigma_y = 115$ μm is pretty close to our detector R&D target and EIC requirement of a spatial resolution in the azimuthal direction of $\sim 100\,\mu m$ for EIC forward tracker. In fact we are confident that we would have achieved an even better resolution $\sigma_y \leq 100\,\mu m$ with a much better quality of the U-V strips readout layer. In the radial direction, the measured resolution of $\sigma_x = 426$ μm actually far exceeds the EIC requirement ~ 1 mm.

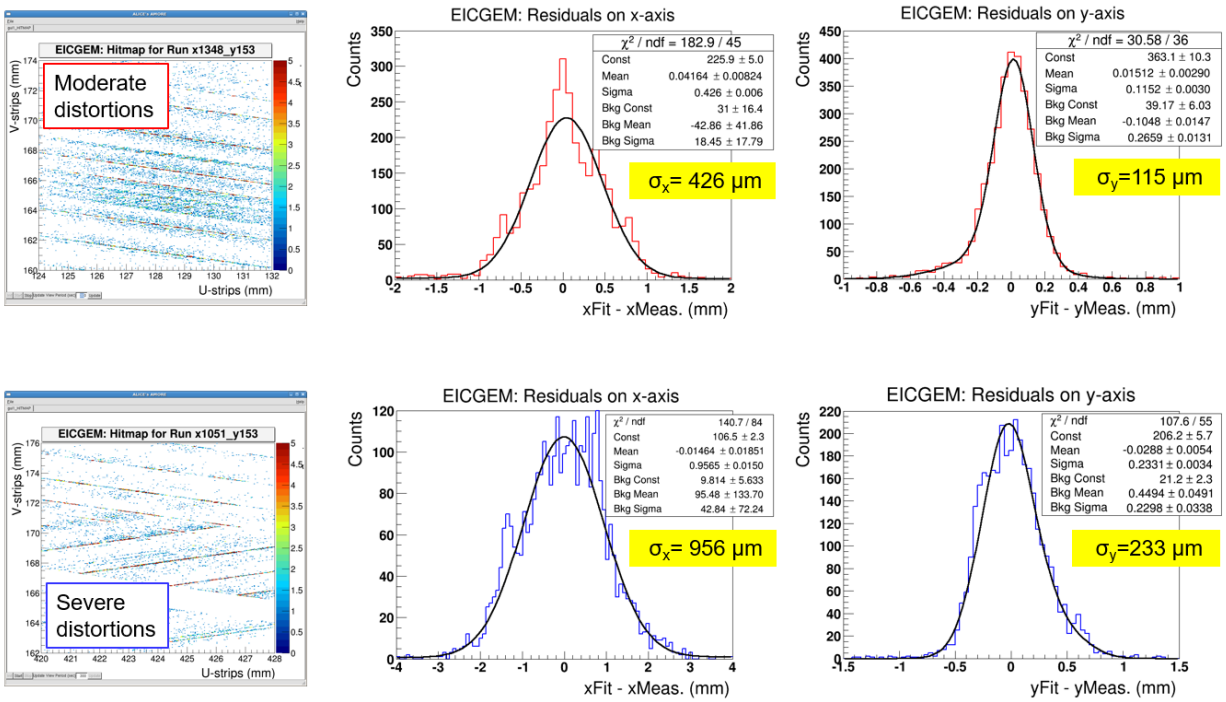

Figure 40: Residual distribution in x *(left:)* and y *(right:)* from the proton beam at two locations on the large GEM prototype and for moderate strip distortions area *(top plots)* and severe strip distortions area *(bottom plots)* on the large GEM prototype.

On the bottom plots of Fig. 40, we can see the residuals in the area of the detector where we observe severe distortions of the reconstructed data and as expected, the resolution in both direction x and y is twice worst than in the moderate distortions area with the width σ roughly the double. Once again, this is just a technical issue with production quality that would be easily fixed in the future. The spatial resolution analysis is ongoing and we expect to refine these results in preparation for the manuscript to be submitted to a peer-reviewed journal later this year.

μRWELL prototype with 2D X-Y strips readout

Characterization with Cosmics: The UVa small size (10×10 cm^2) μRWELL prototype with 2D X-Y strips readout was tested with cosmic in the lab to study the basic characteristics of the detector. The picture on top left of Fig. 41 shows the PCB board with the μRWELL amplification layer glued to the 2D X-Y strips readout layer. Unlike the typical COMPASS 2D strips readout, for this prototype, the copper layer for the top and bottom strips are etched on either side of a 50 μm thick glass epoxy layer and the charges are shared between top and bottom strips through capacitance coupling. This is illustrated in the cross section sketch of μRWELL prototype on top right of Fig. 41. Charge sharing correlation and the ADC distribution plots on top (X-strips) and bottom (Y-strips) layer are shown respectively on the bottom left, center and right of Fig. 41. Signal on the Y-strips are slightly higher than on X-strips.

Fermilab beam test results: At Fermilab beam test, this summer, we set up a one day run dedicated to the study of the μRWELL and the 2D zigzag GEM prototypes during which the small detectors were also installed on the X-Y moving table behind the large EIC prototype as shown on top left of Fig. 42. For this run, we collected data from position scan with the 120GeV proton beam and perform HV scan to determine optimal parameters such as the electric field in the drift volume and μRWELL amplification layer of the

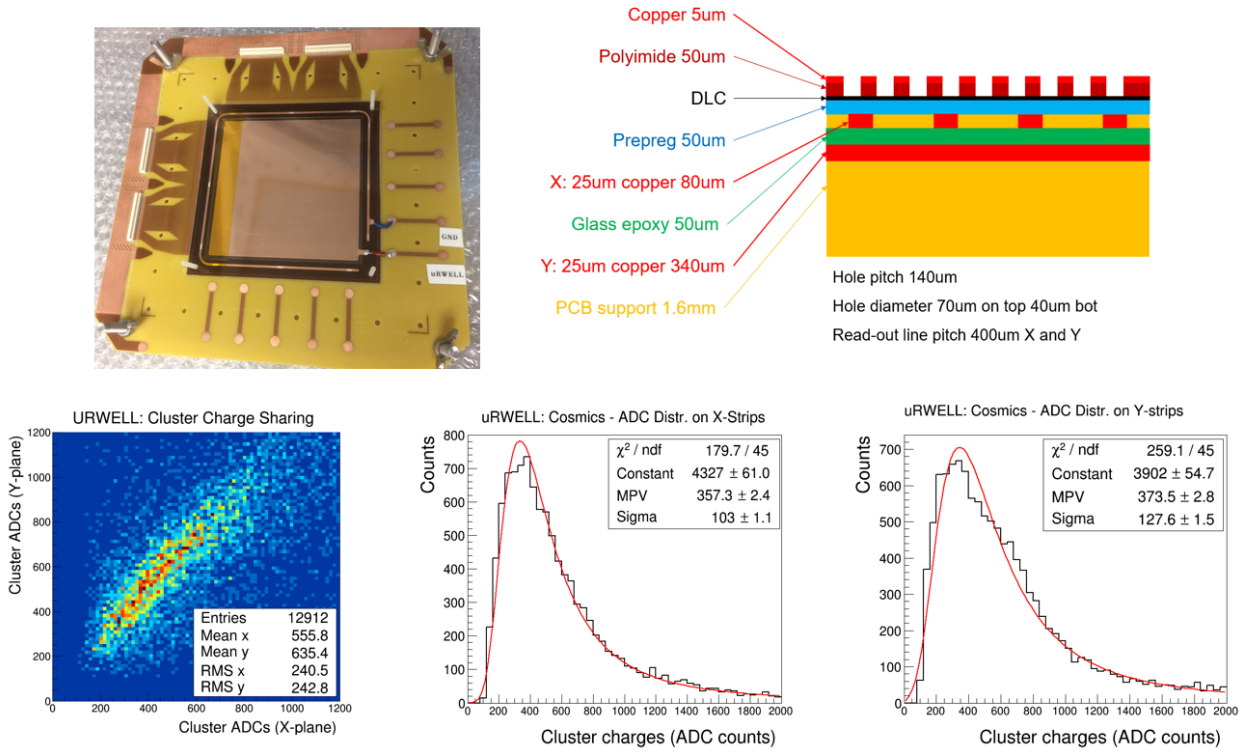

Figure 41: (*Top left:*) μRWELL prototype with 2D X-Y strips readout; *top right:*) Cross section view of the detector; (*bottom left:*) Charge sharing correlation between top layer (X-strips) and bottom layer (Y-strips); (*center*) ADC charge distribution on X-strips (*right* and Y-strips.

μRWELL detector operating with Ar-CO2 (70/30) gas mixture. Fig. 42 (top right) shows the 2D proton beam spots at different locations on the μRWELL detector from the position scan run. The position residual distribution in x and y from the same analysis described above for the large EIC prototype. The width σ_x and σ_y of the residual distribution are respectively equal to 49 μm and 43 μm. σ_y is slightly smaller than σ_x which is also consistent with the slightly unequal charge sharing between x and y strips as we discuss in the paragraph above. Unlike the case for the large EIC GEM where the effect of track fit error in the estimation of the resolution was neglected, for μRWELL prototype, the width of the residuals can not be directly taken as the spatial resolution of the detector. In fact we should reasonably expect a better value for the resolution in the range of 35 to 45 μm in both x and y direction after the track error correction are accounted for. These measured resolution are better than the best results obtained for the spatial resolution for triple-GEM detector of the same size and with similar X-Y strip readout.

2.4 What was not achieved, why not and what will be done to correct?

2.4.1 Brookhaven National Lab

We have not yet measured the TPC prototype equipped with the Micromegas or μRWELL readouts since we've only fairly recently completed the assembly of the prototype equipped with GEMs and have not yet finished the measurements with this setup. However, we have recently received two zigzag PCB's, one coupled to a Micromegas, and the other coupled to a μRWELL. Preliminary testing of these boards has begun with further commissioning tests in planar detector configurations to follow, before these boards are installed in the TPC. In addition, we have not yet read out the TPC prototype with either the SAMPA or DREAM electronics mainly since the setup is new, but more so due to the fact that further work is required to read out these electronics through our data acquisition software. Progress is being made on this front and

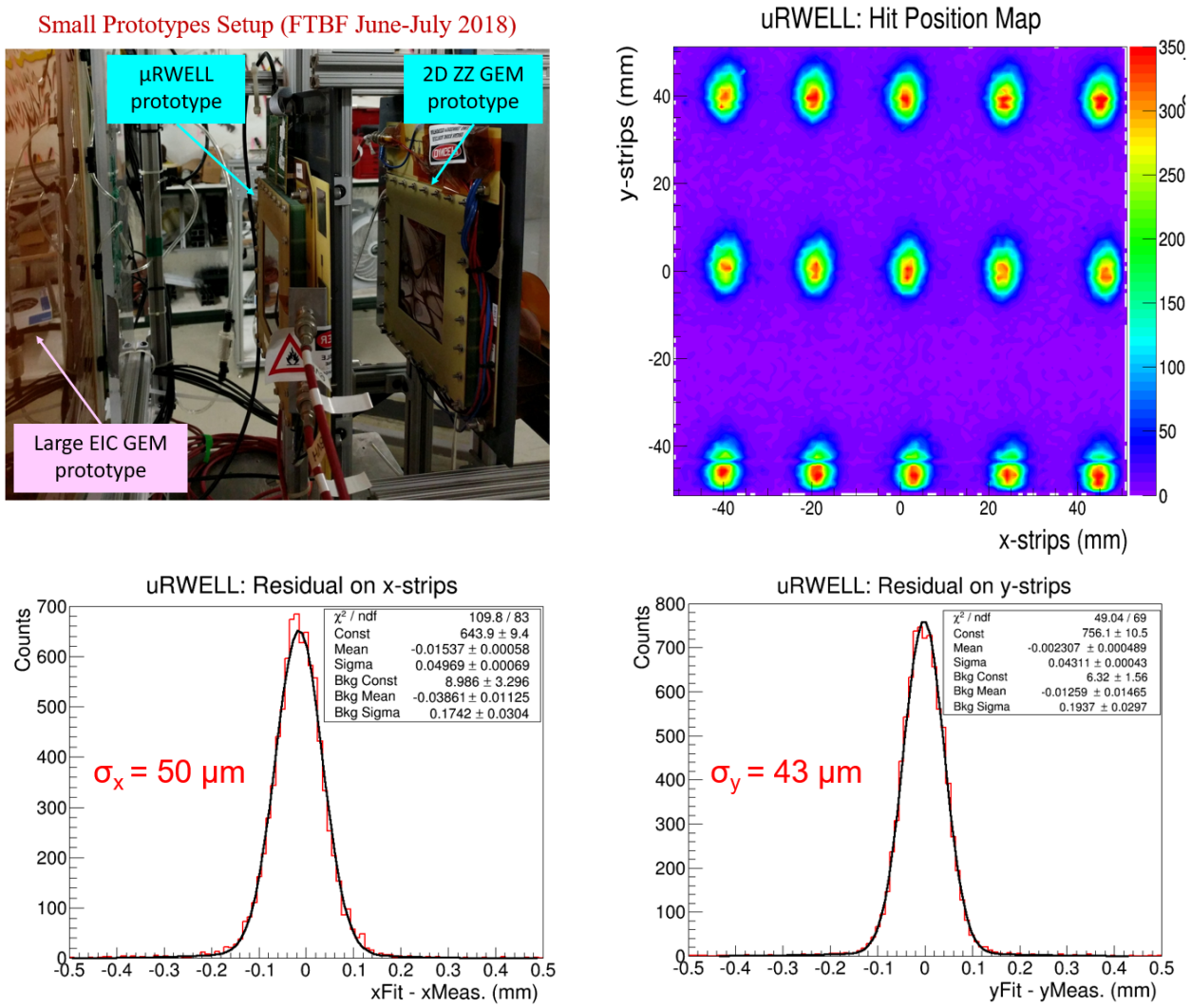

Figure 42: (*Top left:*) Small prototypes setup at Fermilab beam test: μRWELL with X-Y readout and small triple-GEM with 2D zigzag readout installed on the X-Y moving table behind the large EIC GEM; (*top right:*) 2D reconstruction of the proton beam spots from position scan run; (*bottom:*) Residual distribution in x (*left*) and y (*right*) of the μRWELL prototype with the 120 GeV proton beam.

we expect to able to test the TPC with both flavors of electronics during the next funding cycle.

2.4.2 Florida Tech

1. **Forward Tracker Prototype:** Clearly we have not yet been able to characterize the performance of the low-mass prototype due to the observed shorts between foils. Section 2.3.2 above describes in detail how we are attempting to rectify this problem.

2. **μRWELL detector:** Due to the delay with the production and consequently assembly of the $10\times10\,\mathrm{cm}^2$ μRWELL prototype with zigzag-strip readout, we have not yet started designing a first prototype for a small cylindrical μRWELL detector together with UVa. We are hiring a graduate student as a research assistant in the spring semester 2019 to get started on this project.

.

2.4.3 INFN Trieste

The activity is progressing according to planning. Nevertheless, the milestone: "September 2018: The performance of the tests to establish the compatibility of the ND photocathodes with the operation of MPGD-based photon detectors." could not be fully achieved. Some puzzling aspects of the performance observed using THGEM with ND photocathode require repeated exercises of production and test before reaching final conclusions.

2.4.4 Stony Brook University

We invited Prof. Capasso (Harvard University) for a seminar and visit at the facilities at SBU. Prof. Capasso is one of the world experts of meta-material studies and we were hoping to gain insight into the field of meta-materials and maybe collaborate with his group on this topic. The seminar was set to be at SBU on Nov. 9 but had to unfortunately be cancelled due to private commitments of Prof. Capasso on short notice. We have postponed the invitation and hope to make arrangements soon.

2.4.5 Temple University

TU has not yet completed all of its goals for this current funding cycle. In regards to the hardware side, we have our third of four commercial triple-GEM detectors fully assembled, however we have not yet had time to start to fully characterize it (via cosmics/^{55}Fe). We also did not fully assemble the fourth and final commercial triple-GEM detector yet, because we wanted to wait until we tested the third GEM detector first, in case any alterations to the assembly process needed to be made. With the successful test of the third commercial triple-GEM detector, we are now ready to complete the assembly of the forth commercial triple-GEM detector. This will then be followed by testing and characterization of the detector.

TU also has not yet implemented a realistic digitization for the cylindrical shell MPGD operating in a μTPC mode, which prevents a realistic assessment of the tracking performance. This will be the main simulation focus of the remaining funding cycle.

2.4.6 University of Virginia

The design study of small cylindrical μRWELL prototype have not started yet. We have so far concentrated our effort on the Fermilab beam test data analysis.
We have not yet procure the small size VMM-based Scalable Readout System (SRS) as we are waiting for the release of the final and stable version of the VMM-SRS front end cards as well as the other boards of the readout system to place the order.
The drafting of the manuscript on the Chromium GEM (Cr-GEM) results has been going at a very slow pace as we have so far concentrated our efforts on other R&D activities.

3 Future

3.1 What is planned for the next funding cycle and beyond? How, if at all, is this planning different from the original plan?

3.1.1 Brookhaven National Lab

Our proposed R&D activity for the next funding cycle is as follows:

- January - March: Complete the development of the tracking software for the cosmic ray telescope and tune the operating parameters, including the gas gain and DAQ timing for optimal performance. In addition, implement all the necessary calibrations needed to reconstruct particle tracks.
- January - June: Study track reconstruction in the TPC prototype using the cosmic ray telescope and attempt to measure the position resolution and the effective number of primary electrons deposited in the gas (Neff).
- February - June: Read out the TPC with different electronics (ie, SAMPA and DREAM) and attempt to evaluate the performance for each case.
- March - April: Study Micromegas and μRWELL with zigzag readout in a planar detector configuration (ie, short drift gap).
- March - June: Continue work on optimizing the design and production of zigzag readouts in parallel with the eRD6 R&D program.

Long-term goals:

- Further tests with the TPC prototype will include testing zigzag readout patterns optimized for a TPC; testing different different avalanche schemes in the TPC (eg. Micromegas, and μRWELL) ; testing promising gas mixtures; and measuring the charge spread, attachment, and IBF.
- Simulation studies of the response of various zigzag readout patterns in combination with different detector gases and avalanche technologies for a TPC.
- Study the production of "laser tracks" in the drift region of the TPC prtotype. By shooting a UV laser through the UV compatible ports of the TPC enclosure, the TPC gas is ionized along the length of the laser beam via a 2-photon process, which mimics tracks left by minimally ionizing particles. These straight-line pseudo particle tracks may be used as a calibration tool in a full- sized TPC operated at a real experiment, like at the EIC.

These plans are well aligned with our initial goals for this time period.

3.1.2 Florida Tech

1. **Forward Tracker Prototype:** The goal for the next funding period is to assemble the refurbished low-mass prototype and operate it successfully. Then the performance of the low-mass prototype will be characterized with X-rays at Florida Tech, e.g. gain curves. If this succeeds, we will consider a beam test at FNAL in summer 2019.
2. **EIC Simulations:** The next step in this study is to measure the hit residuals for tracks through the chambers by studying the track impact on a dummy plane about 15 cm past the third GEM ring. In this fashion, we will study how the reduction of material in the GEM chambers affects the spread of position values due to multiple scattering. It is expected that the chromium configuration will produce a smaller spread than the standard configuration. This is important for the precision of reconstructing the track impact points on the RICH entrance window that can serve as seeds for RICH ring reconstruction.
3. **μRWELL detector:** We will commission the $10\times10\,\mathrm{cm}^2$ μRWELL prototype with zigzag-strip readout and characterize its performance using X-rays. We plan to begin the design of the first prototype for a small cylindrical μRWELL detector together with UVa.

3.1.3 INFN Trieste

For 2019, we confirm the planning that was presented in June 2018 including two activities.

1. **Single photon detector by MPGD technologies with miniaturized pad-size**.
   The analysis of the data collected at the 2018 test beam exercise where a first version of the prototype will be completed.
   The realization and characterization by laboratory tests of a second version of the prototype is also foreseen. The construction of this second version of the prototype is related to the observed non-uniformity of the gain. As explained in the June 2018 report the source of the effect has been understood: it is related to the design of the anode PCB of the MM multiplication stage. A modified version has already been designed. The construction and characterization of the modified prototype will take place in 2019.

2. **Innovative photocathode based on NanoDiamond (ND) particles**
   The initial studies to understand the compatibility of a photocathode based on NanoDiamond (ND) particles with the operation in gaseous detectors and, in particular, in MPGD-based photon detectors, have been performed in 2018. The characterization of THGEMs with ND coating, both in the case of hydrogenated and non-hydrogenated powder has presented unexpected features, even if very different in the two cases. The 2019 activity will be dedicated to further explore these performance in order to understand the origin of the modified THGEM behavior by producing under controlled parameters a new set of small-size THGEMs, that then will be fully characterized.

Following the activity planning, the **milestones for 2019** are:

- September 2019: The completion of the laboratory characterization of the second version of the photon detector with miniaturized pad-size.
- September 2019: The completion of the studies to understand the performance of THGEMs with ND coating, both in the hydrogenized and non-hydrogenized versions.

3.1.4 Stony Brook University

The test-beam campaign at FTBF has been completed in the first week of July 2018 and the analysis of the TPC-prototype has been finalized. The results were presented at various internal meetings.
We have acquired an X-ray tube setup with a gantry system that allows precisely positioned and controlled illumination of detectors with an almost mono-chromatic source. The devices will be arriving at SBU at the end of January.

The final installation of the evaporator equipment will be performed in the first quarter of 2019 and first commissioning of the system is planned thereafter.

We are planning on continuing the investigation of meta-materials suited for the application of Cherenkov photon detection. We are expecting in January the COMSOL-software we have purchased and need to familiarize ourselves with the operation of the software. Students will be returning by the end of January and we are expecting to model appropriate materials within the first two or three weeks in February.

We are working on making up the invitation of the Prof. Capasso from Harvard University to learn most about meta-materials.

Planned schedule:

- Jan-Mar 2019 IBF measurements
- Jan-Apr 2019 Final evaporator installation

- Feb-May 2019 Simulation of meta-materials
- Apr-May 2019 Evaporator commissioning

3.1.5 Temple University

During the remaining time in this funding period, TU plans on finishing out the R&D related to the commercial triple-GEM detectors. This includes assembling the triple-GEM stack of the fourth and last commercial GEM detector, and characterizing its performance along with the recently assembled third triple-GEM detector. The performance of both detectors will be assessed via cosmic and using an ^{55}Fe source. This will complete the eRD3 carry over R&D.

Additionally, TU will continue work on simulating a MPGD cylindrical detector operating in a μTPC mode. In particular we will focus on implementing a realistic digitization scheme, which will be based on test beam results BNL acquired when testing a μTPC using a Compass readout. With the digitization scheme in place we can then assess accurate tracking performance of such a detector. Additionally we can then look at the tracking impact when including a TPC with the cylindrical MPGD shells, as well as integrating the forward MPGD tracking simulations that FIT is working on. This will allow us to study the global performance of the tracking detectors within the entire EIC phase space.

3.1.6 University of Virginia

Our plans and R&D goals for next cycle of FY19 are:

1. **Large EIC-FT-GEM prototype:** Continue the analysis of the FTBF data. Present the results of the performances of the prototype at MPGD2019 conference in Spring 2019 and start preparing the draft of the manuscript for publication in peer-reviewed journal.
2. **R&D on μRWELL detector technology:** Continue the work on the design of a small cylindrical μRWELL detector with FIT and TU. Procure a second 10 cm $\times$ 10 cm prototype with the R&D focus on low mass and high resolution 2D readout strips patterns. We will also continue the study and characterization of our current small prototype and most importantly the performance of this new technology in high particle rate environment.
3. **VMM readout electronics:** Procure a small size VMM-based Scalable Readout System (SRS) if a stable version of the FE cards are available and start testing this new electronics with the our detectors to compare the performances of VMM-SRS readout system with the APV25 electronics.
4. **Draft paper on Chromium GEM (Cr-GEM) studies:** Continue working on the draft paper for the publication of the results in NIMA or TNS journal.

3.2 What are the critical issues?

3.2.1 Brookhaven National Lab

There are no technical issues that would impede our progress towards reaching our goals for the next funding cycle. However, broadly speaking, up to this point we have concentrated our efforts on optimizing various forms of readout for planar (short drift) detectors. A critical issue we face is the optimization of the readout of the TPC, which includes significant variability in the size of charge clouds impinging the readout plane due to transverse diffusion over relatively long drift distances. Specifically, the particular zigzag patterns employed and the GEM field configurations that were found to be well suited for planar detectors are likely not optimal for TPC applications. Therefore, it is urgent to investigate the response of the TPC for

different zigzag patterns and operating parameters for the avalanche scheme. This includes investigating the implementation of Micromegas and μRWELL.

3.2.2 Florida Tech

Technical Issues: For the low-mass forward tracker prototype it is critical to demonstrate that the mechanical foil stretching technique using a carbon fiber frame is a viable design that leads to an operable detector.

Manpower Issues: The departure of our post-doc Aiwu Zhang back in December 2016 is still severely slowing down progress. While our undergraduates are doing a fine job and are very enthusiastic about building and testing prototype detectors and simulating a forward GEM tracker, they have limited availability and experience. For the simulation work it is critical for our students to receive continued support from EicRoot experts at BNL to develop enough expertise with EicRoot so that they can analyze tracking performance and use it for studying the impact of multiple scattering on forward tracks. We need additional manpower to get started on the design of the cylindrical μRWELL detector. Consequently, we will be shifting a graduate student toward that work and fund his stipend through the EIC R&D project.

3.2.3 INFN Trieste

No technical critical issue is expected for the completion of the planed 2019 activity.

Nevertheless, the exploratory exercises concerning the photocathodes based on ND material can deserve surprises related to the high innovative approach. The progress rate can be affected by these possible surprises.

3.2.4 Stony Brook University

No critical issues have been identified.

3.2.5 Temple University

No critical issues.

3.2.6 University of Virginia

No critical issues.

4 Manpower

4.1 Brookhaven National Lab

This work is being carried out by members of the BNL Physics Department. It includes two Senior Scientists (0.2 FTE), two Physics Associates (1.2 FTE), and one Technician (0.3 FTE).

4.2 Florida Tech

- Marcus Hohlmann, Professor, 0.25 FTE, not funded under this R&D program.
- Sarah Arends, physics undergraduate student, μRWELL prototype assembly, not funded.
- Matthew Bomberger, physics undergraduate student, EicRoot simulation and low-mass forward tracker prototype, not funded.
- Jacob Chesslo, physics undergraduate student, design of new inner frames for forward tracker prototype, not funded.
- Jacqui Miksanek, physics undergraduate student, μRWELL prototype assembly, not funded.
- Akshath Wikramanayake, physics undergraduate student, EicRoot simulation, not funded.

4.3 INFN Trieste

From INFN Trieste:

- C. Chatterjee (Trieste University and INFN, PhD student)
- S. Dalla Torre (INFN, Staff)
- S. Dasgupta (INFN, postdoc)
- S. Levorato (INFN, staff)
- Triloki (ICTP, postdoc)
- F. Tessarotto (INFN, Staff)
- Y. Zhao (INFN, postdoc)

The contribution of technical personnel from INFN-Trieste is also foreseen according to needs.

From INFN BARI:

- Grazia Cicala (NCR staff and INFN)
- Antonio Valentini (Bari University and INFN, professor)

Globally, the dedicated manpower is equivalent to 3 FTE.

4.4 Stony Brook University

- K. Dehmelt, Research Scientist, 0.3 FTE
- T. K. Hemmick, Professor, 0.1 FTE
- P. Garg, Postdoc, 0.1 FTE

We have no personnel funded under this R&D program.

4.5 Temple University

Temple University's workforce is listed below:

- B. Surrow; Professor; 0.1 FTE
- M. Posik; Assistant Research Professor; 0.2 FTE
- A. Quintero; Post-doc ; 0.3 FTE

4.6 University of Virginia

None of the labor at UVa is funded by EIC R&D. The workforce is listed below:

- N. Liyanage; Professor; 0.1 FTE
- K. Gnanvo; Research Scientist; 0.5 FTE

5 External Funding

5.1 Brookhaven National Lab

All scientific manpower at BNL would be provided by internal funding. However, technician and designer labor would need to be supported through EIC R&D funds.

Additional R&D work on Micropattern Detectors for EIC is also being provided by a BNL LDRD in collaboration with Saclay and Stony Brook. This is supporting our continued work on zigzag readout with GEMs and Micromegas and we do not request any funding for this effort from EIC R&D funds. However, our proposed work on TPC R&D for EIC would not be covered under LDRD funds.

5.2 Florida Tech

None.

5.3 INFN Trieste

INFN has assigned to this activity a support of 11.5 keuro for the year 2019.

5.4 Stony Brook University

There is no external funding for this R&D effort.

5.5 Temple University

None.

5.6 University of Virginia

UVa has DOE basic research grant from Medium Energy Physics. The R&D work on Cr-GEM is partly funded with the research grant.

References

[1] B. Azmoun et al. "A Study of a Mini-Drift GEM Tracking Detector". In: *IEEE Transactions on Nuclear Science* 63.3 (June 2016), pp. 1768–1776. ISSN: 0018-9499. DOI: 10.1109/TNS.2016.2550503.

[2] Craig Woody et al. "A Prototype Combination TPC Cherenkov Detector with GEM Readout for Tracking and Particle Identification and its Potential Use at an Electron Ion Collider". In: 2015. arXiv: 1512.05309 [physics.ins-det]. URL: https://inspirehep.net/record/1409973/files/arXiv:1512.05309.pdf.

[3] B. Azmoun et al. "Design Studies for a TPC Readout Plane Using Zigzag Patterns with Multistage GEM Detectors". In: *IEEE Transactions on Nuclear Science* (July 2018), pp. 1–1. ISSN: 0018-9499. DOI: 10.1109/TNS.2018.2846403.

[4] Aiwu Zhang et al. "Performance of a Large-area GEM Detector Read Out with Wide Radial Zigzag Strips". In: *Nucl. Instrum. Meth.* A811 (2016), pp. 30–41. DOI: 10.1016/j.nima.2015.11.157. arXiv: 1508.07046 [physics.ins-det].

[5] Aiwu Zhang et al. "A GEM readout with radial zigzag strips and linear charge-sharing response". In: *Nucl. Instrum. Meth.* A887 (2018), pp. 184–192. arXiv: 1708.07931 [physics.ins-det].

[6] Marcus Hohlmann et al. "Low-mass GEM detector with radial zigzag readout strips for forward tracking at the EIC". In: *2017 IEEE Nuclear Science Symposium and Medical Imaging Conference (NSS/MIC 2017) Atlanta, Georgia, USA, October 21-28, 2017*. 2017. arXiv: 1711.05333 [physics.ins-det]. URL: http://inspirehep.net/record/1636290/files/arXiv:1711.05333.pdf.

[7] E. Albrecht et al. "Status and characterisation of COMPASS RICH-1". In: *Nuclear Instruments and Methods in Physics Research Section A: Accelerators, Spectrometers, Detectors and Associated Equipment* 553.1 (2005). Proceedings of the fifth International Workshop on Ring Imaging Detectors, pp. 215–219. ISSN: 0168-9002. DOI: https://doi.org/10.1016/j.nima.2005.08.036. URL: http://www.sciencedirect.com/science/article/pii/S0168900205016001.

[8] P. Abbon et al. "Read-out electronics for fast photon detection with COMPASS RICH-1". In: *Nuclear Instruments and Methods in Physics Research Section A: Accelerators, Spectrometers, Detectors and Associated Equipment* 587.2 (2008), pp. 371–387. ISSN: 0168-9002. DOI: https://doi.org/10.1016/j.nima.2007.12.026. URL: http://www.sciencedirect.com/science/article/pii/S0168900207024576.

[9] P. Abbon et al. "Design and construction of the fast photon detection system for COMPASS RICH-1". In: *Nuclear Instruments and Methods in Physics Research Section A: Accelerators, Spectrometers, Detectors and Associated Equipment* 616.1 (2010), pp. 21–37. ISSN: 0168-9002. DOI: https://doi.org/10.1016/j.nima.2010.02.069. URL: http://www.sciencedirect.com/science/article/pii/S0168900210002676.

[10] P. Abbon et al. "Particle identification with COMPASS RICH-1". In: *Nuclear Instruments and Methods in Physics Research Section A: Accelerators, Spectrometers, Detectors and Associated Equipment* 631.1 (2011), pp. 26–39. ISSN: 0168-9002. DOI: https://doi.org/10.1016/j.nima.2010.11.106. URL: http://www.sciencedirect.com/science/article/pii/S0168900210026422.

[11] P. Abbon et al. "The COMPASS experiment at CERN". In: *Nuclear Instruments and Methods in Physics Research Section A: Accelerators, Spectrometers, Detectors and Associated Equipment* 577.3 (2007), pp. 455–518. ISSN: 0168-9002. DOI: https://doi.org/10.1016/j.nima.2007.03.026. URL: http://www.sciencedirect.com/science/article/pii/S0168900207005001.

[12] P. Abbon et al. "The COMPASS setup for physics with hadron beams". In: *Nuclear Instruments and Methods in Physics Research Section A: Accelerators, Spectrometers, Detectors and Associated Equipment* 779.Supplement C (2015), pp. 69–115. ISSN: 0168-9002. DOI: https://doi.org/10.1016/j.nima.2015.01.035. URL: http://www.sciencedirect.com/science/article/pii/S0168900215000662.

[13] M. Alexeev et al. "The quest for a third generation of gaseous photon detectors for Cherenkov imaging counters". In: *Nuclear Instruments and Methods in Physics Research Section A: Accelerators, Spectrometers, Detectors and Associated Equipment* 610.1 (2009). New Developments In Photodetection NDIP08, pp. 174–177. ISSN: 0168-9002. DOI: https://doi.org/10.1016/j.nima.2009.05.069. URL: http://www.sciencedirect.com/science/article/pii/S0168900209010560.

[14] M. Alexeev et al. "THGEM based photon detector for Cherenkov imaging applications". In: *Nuclear Instruments and Methods in Physics Research Section A: Accelerators, Spectrometers, Detectors and Associated Equipment* 617.1 (2010). 11th Pisa Meeting on Advanced Detectors, pp. 396–397. ISSN: 0168-9002. DOI: https://doi.org/10.1016/j.nima.2009.08.087. URL: http://www.sciencedirect.com/science/article/pii/S0168900209017173.

[15] M. Alexeev et al. "Micropattern gaseous photon detectors for Cherenkov imaging counters". In: *Nuclear Instruments and Methods in Physics Research Section A: Accelerators, Spectrometers, Detectors and Associated Equipment* 623.1 (2010). 1st International Conference on Technology and Instrumentation in Particle Physics, pp. 129–131. ISSN: 0168-9002. DOI: https://doi.org/10.1016/j.nima.2010.02.171. URL: http://www.sciencedirect.com/science/article/pii/S0168900210004389.

[16] M. Alexeev et al. "Development of THGEM-based Photon Detectors for COMPASS RICH-1". In: *Phys. Procedia* 37 (2012), pp. 781–788. DOI: 10.1016/j.phpro.2012.02.422.

[17] M Alexeev et al. "Development of THGEM-based photon detectors for Cherenkov Imaging Counters". In: *Journal of Instrumentation* 5.03 (2010), P03009. URL: http://stacks.iop.org/1748-0221/5/i=03/a=P03009.

[18] M. Alexeev et al. "Progress towards a THGEM-based detector of single photons". In: *Nuclear Instruments and Methods in Physics Research Section A: Accelerators, Spectrometers, Detectors and Associated Equipment* 639.1 (2011). Proceedings of the Seventh International Workshop on Ring Imaging Cherenkov Detectors, pp. 130–133. ISSN: 0168-9002. DOI: https://doi.org/10.1016/j.nima.2010.10.117. URL: http://www.sciencedirect.com/science/article/pii/S0168900210024022.

[19] M. Alexeev et al. "Detection of single photons with THickGEM-based counters". In: *Nuclear Instruments and Methods in Physics Research Section A: Accelerators, Spectrometers, Detectors and Associated Equipment* 695.Supplement C (2012). New Developments in Photodetection NDIP11, pp. 159–162. ISSN: 0168-9002. DOI: https://doi.org/10.1016/j.nima.2011.11.079. URL: http://www.sciencedirect.com/science/article/pii/S0168900211021498.

[20] M Alexeev et al. "Detection of single photons with ThickGEM-based counters". In: *Journal of Instrumentation* 7.02 (2012), p. C02014. URL: http://stacks.iop.org/1748-0221/7/i=02/a=C02014.

[21] M. Alexeev et al. "Detection of single photons with hybrid ThickGEM-based counters". In: *PoS* PhotoDet2012 (2012), p. 057.

[22] M. Alexeev et al. "THGEM-based photon detectors for the upgrade of COMPASS RICH-1". In: *Nuclear Instruments and Methods in Physics Research Section A: Accelerators, Spectrometers, Detectors and Associated Equipment* 732.Supplement C (2013). Vienna Conference on Instrumentation 2013, pp. 264–268. ISSN: 0168-9002. DOI: https://doi.org/10.1016/j.nima.2013.08.020. URL: http://www.sciencedirect.com/science/article/pii/S0168900213011467.

[23] M Alexeev et al. "Status and progress of novel photon detectors based on THGEM and hybrid MPGD architectures". In: *Journal of Instrumentation* 8.12 (2013), p. C12005. URL: http://stacks.iop.org/1748-0221/8/i=12/a=C12005.

[24] M Alexeev et al. "Ion backflow in thick GEM-based detectors of single photons". In: *Journal of Instrumentation* 8.01 (2013), P01021. URL: http://stacks.iop.org/1748-0221/8/i=01/a=P01021.

[25] M. Alexeev et al. "Status and progress of the novel photon detectors based on THGEM and hybrid MPGD architectures". In: *Nuclear Instruments and Methods in Physics Research Section A: Accelerators, Spectrometers, Detectors and Associated Equipment* 766.Supplement C (2014). RICH2013 Proceedings of the Eighth International Workshop on Ring Imaging Cherenkov Detectors Shonan, Kanagawa, Japan, December 2-6, 2013, pp. 133–137. ISSN: 0168-9002. DOI: https://doi.org/10.1016/j.nima.2014.07.030. URL: http://www.sciencedirect.com/science/article/pii/S0168900214008730.

[26] M Alexeev et al. "Progresses in the production of large-size THGEM boards". In: *Journal of Instrumentation* 9.03 (2014), p. C03046. URL: http://stacks.iop.org/1748-0221/9/i=03/a=C03046.

[27] M Alexeev et al. "MPGD-based counters of single photons developed for COMPASS RICH-1". In: *Journal of Instrumentation* 9.09 (2014), p. C09017. URL: http://stacks.iop.org/1748-0221/9/i=09/a=C09017.

[28] Stefano Levorato et al. "MPGD-based counters of single photons for Cherenkov imaging counters." In: *PoS* TIPP2014 (2014), p. 075.

[29] M. Alexeev et al. "The gain in Thick GEM multipliers and its time-evolution". In: *Journal of Instrumentation* 10.03 (2015), P03026. URL: http://stacks.iop.org/1748-0221/10/i=03/a=P03026.

[30] M. Alexeev et al. "Status of the development of large area photon detectors based on THGEMs and hybrid MPGD architectures for Cherenkov imaging applications". In: *Nuclear Instruments and Methods in Physics Research Section A: Accelerators, Spectrometers, Detectors and Associated Equipment* 824.Supplement C (2016). Frontier Detectors for Frontier Physics: Proceedings of the 13th Pisa Meeting on Advanced Detectors, pp. 139–142. ISSN: 0168-9002. DOI: https://doi.org/10.1016/j.nima.2015.11.034. URL: http://www.sciencedirect.com/science/article/pii/S0168900215013996.

[31] G. Hamar et al. "Investigation of the properties of Thick-GEM photocathodes by microscopic scale measurements with single photo-electrons". In: *Nuclear Instruments and Methods in Physics Research Section A: Accelerators, Spectrometers, Detectors and Associated Equipment* 876.Supplement C (2017). The 9th international workshop on Ring Imaging Cherenkov Detectors (RICH2016), pp. 233–236. ISSN: 0168-9002. DOI: https://doi.org/10.1016/j.nima.2017.03.016. URL: http://www.sciencedirect.com/science/article/pii/S0168900217303534.

[32] M. Alexeev et al. "The MPGD-based photon detectors for the upgrade of COMPASS RICH-1". In: *Nuclear Instruments and Methods in Physics Research Section A: Accelerators, Spectrometers, Detectors and Associated Equipment* 876.Supplement C (2017). The 9th international workshop on Ring Imaging Cherenkov Detectors (RICH2016), pp. 96–100. ISSN: 0168-9002. DOI: https://doi.org/10.1016/j.nima.2017.02.013. URL: http://www.sciencedirect.com/science/article/pii/S0168900217301936.

[33] G. Hamar et al. "MPGD-based photon detector upgrade for COMPASS RICH". In: *Journal of Instrumentation* 12.07 (2017), p. C07026. URL: http://stacks.iop.org/1748-0221/12/i=07/a=C07026.

[34] J. Agarwala et al. "Novel MPGD based detectors of single photons in COMPASS RICH-1". In: *Nuclear Instruments and Methods in Physics Research Section A: Accelerators, Spectrometers, Detectors and Associated Equipment* (2017). ISSN: 0168-9002. DOI: https://doi.org/10.1016/j.nima.2017.11.011. URL: http://www.sciencedirect.com/science/article/pii/S016890021731197X.

[35] J. Agarwala et al. "The MPGD-based photon detectors for the upgrade of COMPASS RICH-1 and beyond". In: *Nuclear Instruments and Methods in Physics Research Section A: Accelerators, Spectrometers, Detectors and Associated Equipment* (2018). ISSN: 0168-9002. DOI: https://doi.org/10.1016/j.nima.2018.10.092. URL: http://www.sciencedirect.com/science/article/pii/S0168900218314062.

[36] Luciano Velardi, Antonio Valentini, and Grazia Cicala. "UV photocathodes based on nanodiamond particles: Effect of carbon hybridization on the efficiency". In: *Diamond and Related Materials* 76.Supplement C (2017), pp. 1–8. ISSN: 0925-9635. DOI: https://doi.org/10.1016/j.diamond.2017.03.017. URL: http://www.sciencedirect.com/science/article/pii/S0925963516306999.

[37] B. Surrow. "The STAR Forward GEM Tracker". In: *Nucl. Instrum. Meth A* 617 (2010), p. 196. DOI: 10.1016/j.nima.2009.09.012.

[38] Kondo Gnanvo et al. "Performance in test beam of a large-area and light-weight GEM detector with 2D stereo-angle (UV) strip readout". In: *Nucl. Instrum. Meth.* A808 (2016), pp. 83–92. DOI: 10.1016/j.nima.2015.11.071. arXiv: 1509.03875 [physics.ins-det].

[39] S Martoiu et al. "Development of the scalable readout system for micro-pattern gas detectors and other applications". In: *Journal of Instrumentation* 8.03 (2013), p. C03015. URL: http://stacks.iop.org/1748-0221/8/i=03/a=C03015.

[40] J. Agarwala et al. "Optimized MPGD-based Photon Detectors for high momentum particle identification at the Electron-Ion Collider". In: *Nuclear Instruments and Methods in Physics Research Section A: Accelerators, Spectrometers, Detectors and Associated Equipment* (2018). ISSN: 0168-9002. DOI: https://doi.org/10.1016/j.nima.2018.10.185. URL: http://www.sciencedirect.com/science/article/pii/S0168900218314992.

[41] J. Agarwala et al. "Novel NanoDiamond based photocathodes for gaseous detectors". In: 2018. arXiv: 1812.04552 [physics.ins-det].

[42] Ginis V. et al. "Controlling Cherenkov Radiation with Transformation-Optical Metamaterials". In: *Physical Review Letters* 113.167402 (2014). DOI: 10.1103/PhysRevLett.113.167402.

A List of all EIC publications from the eRD6 Consortium

BNL publications:

[1] B. Azmoun et al. "Design Studies for a TPC Readout Plane Using Zigzag Patterns with Multistage GEM Detectors". In: *IEEE Transactions on Nuclear Science* (July 2018), pp. 1–1. ISSN: 0018-9499. DOI: 10.1109/TNS.2018.2846403.

[2] B. Azmoun et al. "A Study of a Mini-Drift GEM Tracking Detector". In: *IEEE Transactions on Nuclear Science* 63.3 (June 2016), pp. 1768–1776. ISSN: 0018-9499. DOI: 10.1109/TNS.2016.2550503.

[3] Craig Woody et al. "A Prototype Combination TPC Cherenkov Detector with GEM Readout for Tracking and Particle Identification and its Potential Use at an Electron Ion Collider". In: 2015. arXiv: 1512.05309 [physics.ins-det]. URL: https://inspirehep.net/record/1409973/files/arXiv:1512.05309.pdf.

[4] B. Azmoun et al. "Initial studies of a short drift GEM tracking detector". In: *2014 IEEE Nuclear Science Symposium and Medical Imaging Conference (NSS/MIC)*. Nov. 2014, pp. 1–2. DOI: 10.1109/NSSMIC.2014.7431059.

[5] M. L. Purschke et al. "Test beam study of a short drift GEM tracking detector". In: *2013 IEEE Nuclear Science Symposium and Medical Imaging Conference (2013 NSS/MIC)*. Oct. 2013, pp. 1–4. DOI: 10.1109/NSSMIC.2013.6829463.

Florida Tech publications:

[1] Marcus Hohlmann et al. "Low-mass GEM detector with radial zigzag readout strips for forward tracking at the EIC". In: *2017 IEEE Nuclear Science Symposium and Medical Imaging Conference (NSS/MIC 2017) Atlanta, Georgia, USA, October 21-28, 2017*. 2017. arXiv: 1711.05333 [physics.ins-det]. URL: http://inspirehep.net/record/1636290/files/arXiv:1711.05333.pdf.

[2] Aiwu Zhang et al. “A GEM readout with radial zigzag strips and linear charge-sharing response”. In: *Nucl. Instrum. Meth.* A887 (2018), pp. 184–192. arXiv: 1708.07931 [physics.ins-det].

[3] Aiwu Zhang and Marcus Hohlmann. “Accuracy of the geometric-mean method for determining spatial resolutions of tracking detectors in the presence of multiple Coulomb scattering”. In: *JINST* 11.06 (2016), P06012. DOI: 10.1088/1748-0221/11/06/P06012. arXiv: 1604.06130 [physics.data-an].

[4] Aiwu Zhang et al. “R&D on GEM detectors for forward tracking at a future Electron-Ion Collider”. In: *Proceedings, 2015 IEEE Nuclear Science Symposium and Medical Imaging Conference (NSS/MIC 2015): San Diego, California, United States*. 2016, p. 7581965. DOI: 10.1109/NSSMIC.2015.7581965. arXiv: 1511.07913 [physics.ins-det]. URL: http://inspirehep.net/record/1406551/files/arXiv:1511.07913.pdf.

[5] Aiwu Zhang et al. “Performance of a Large-area GEM Detector Read Out with Wide Radial Zigzag Strips”. In: *Nucl. Instrum. Meth.* A811 (2016), pp. 30–41. DOI: 10.1016/j.nima.2015.11.157. arXiv: 1508.07046 [physics.ins-det].

INFN publications:

[1] J. Agarwala et al. “Optimized MPGD-based Photon Detectors for high momentum particle identification at the Electron-Ion Collider”. In: *Nuclear Instruments and Methods in Physics Research Section A: Accelerators, Spectrometers, Detectors and Associated Equipment* (2018). ISSN: 0168-9002. DOI: https://doi.org/10.1016/j.nima.2018.10.185. URL: http://www.sciencedirect.com/science/article/pii/S0168900218314992.

[2] J. Agarwala et al. “Novel NanoDiamond based photocathodes for gaseous detectors”. In: 2018. arXiv: 1812.04552 [physics.ins-det].

SBU publications:

[1] M. Blatnik et al. “Performance of a Quintuple-GEM Based RICH Detector Prototype”. In: *IEEE Trans. Nucl. Sci.* 62.6 (2015), pp. 3256–3264. DOI: 10.1109/TNS.2015.2487999. arXiv: 1501.03530 [physics.ins-det].

TU publications:

[1] M. Posik and B. Surrow. “Construction of a Triple-GEM Detector Using Commercially Manufactured Large GEM Foils”. In: 2018. arXiv: 1806.01892 [physics.ins-det].

[2] M. Posik and B. Surrow. “Construction of Triple-GEM Detectors Using Commercially Manufactured Large GEM Foils”. In: *Proceedings, 2016 IEEE Nuclear Science Symposium and Medical Imaging Conference: NSS/MIC 2016: Strasbourg, France*. 2016, p. 8069743. DOI: 10.1109/NSSMIC.2016.8069743. arXiv: 1612.03776 [physics.ins-det].

[3] M. Posik and B. Surrow. “Optical and electrical performance of commercially manufactured large GEM foils”. In: *Nucl. Instrum. Meth.* A802 (2015), pp. 10–15. DOI: 10.1016/j.nima.2015.08.048. arXiv: 1506.03652 [physics.ins-det].

[4] M. Posik and B. Surrow. “R&D of commercially manufactured large GEM foils”. In: *Proceedings, 2015 IEEE Nuclear Science Symposium and Medical Imaging Conference (NSS/MIC 2015): San Diego, California, United States*. 2016, p. 7581802. DOI: 10.1109/NSSMIC.2015.7581802. arXiv: 1511.08693 [physics.ins-det].

[5] M. Posik and B. Surrow. "Research and Development of Commercially Manufactured Large GEM Foils". In: *Proceedings, 21st Symposium on Room-Temperature Semiconductor X-ray and Gamma-ray Detectors (RTSD 2014): Seattle, WA, USA, November 8-15, 2014*. 2016, p. 7431060. DOI: 10.1109/NSSMIC.2014.7431060. arXiv: 1411.7243 [physics.ins-det].

UVa publications:

[1] Kondo Gnanvo et al. "Large Size GEM for Super Bigbite Spectrometer (SBS) Polarimeter for Hall A 12 GeV program at JLab". In: *Nucl. Instrum. Meth.* A782 (2015), pp. 77–86. DOI: 10.1016/j.nima.2015.02.017. arXiv: 1409.5393 [physics.ins-det].

[2] Kondo Gnanvo et al. "Performance in test beam of a large-area and light-weight GEM detector with 2D stereo-angle (UV) strip readout". In: *Nucl. Instrum. Meth.* A808 (2016), pp. 83–92. DOI: 10.1016/j.nima.2015.11.071. arXiv: 1509.03875 [physics.ins-det].

Yale publications:

[1] S. Aiola et al. "Combination of two Gas Electron Multipliers and a Micromegas as gain elements for a time projection chamber". In: *Nucl. Instrum. Meth.* A834 (2016), pp. 149–157. DOI: 10.1016/j.nima.2016.08.007. arXiv: 1603.08473 [physics.ins-det].